Available online at www.sciencedirect.com
ScienceDirect
Journal of Sound and Vibration 311 (2008) 1075–1099
JOURNAL OF SOUND AND VIBRATION
www.elsevier.com/locate/jsvi

Response-only method for damage detection of beam-like structures using high accuracy frequencies with auxiliary mass spatial probing

Shuncong Zhong[a], S. Olutunde Oyadiji[a,*], Kang Ding[b]

[a]*Dynamics and Aeroelasticity Research Group, School of Mechanical, Aerospace and Civil Engineering, The University of Manchester, Manchester M13 9PL, UK*
[b]*Faculty of Automobile Engineering, South China University of Technology, PR China*

Received 16 October 2006; received in revised form 28 September 2007; accepted 2 October 2007
Available online 21 December 2007

Abstract

This paper proposes a new approach based on auxiliary mass spatial probing using spectral centre correction method (SCCM), to provide a simple solution for damage detection by just using the response time history of beam-like structures. The natural frequencies of a damaged beam with a traversing auxiliary mass change due to change in the inertia of the beam as the auxiliary mass is traversed along the beam, as well as the point-to-point variations in the flexibility of the beam. Therefore the auxiliary mass can enhance the effects of the crack on the dynamics of the beam and, therefore, facilitate the identification and location of damage in the beam. That is, the auxiliary mass can be used to probe the dynamic characteristic of the beam by traversing the mass from one end of the beam to the other. However, it is impossible to obtain accurate modal frequencies by the direct operation of the fast Fourier transform (FFT) of the response data of the structure because the frequency spectrum can be only calculated from limited sampled time data which results in the well-known leakage effect. SCCM is identical to the energy centrobaric correction method (ECCM) which is a practical and effective method used in rotating mechanical fault diagnosis and which resolves the shortcoming of FFT and can provide high accuracy estimate of frequency, amplitude and phase. In the present work, the modal responses of damaged simply supported beams with auxiliary mass are computed using the finite element method (FEM). The graphical plots of the natural frequencies calculated by SCCM versus axial location of auxiliary mass are obtained. However, it is difficult to locate the crack directly from the curve of natural frequencies. A simple and fast method, the derivatives of natural frequency curve, is proposed in the paper which can provide crack information for damage detection of beam-like structures. The efficiency and practicability of the proposed method is illustrated via numerical simulation. For real cases, experimental noise is expected to corrupt the response data and, ultimately, the natural frequencies of beam-like structures. Therefore, the response data with a normally distributed random noise is also studied. Also, the effects of crack depth, auxiliary mass and damping ratios on the proposed method are investigated. From the simulated results, the efficiency and robustness of the proposed method is demonstrated. The results show that the proposed method has low computational cost and high precision.

*Corresponding author. Tel.: +44 161 275 4348; fax: +44 161 275 3844.
E-mail address: s.o.oyadiji@manchester.ac.uk (S.O. Oyadiji).

0022-460X/$ - see front matter © 2007 Elsevier Ltd. All rights reserved.
doi:10.1016/j.jsv.2007.10.004

1. Introduction

The initiation and propagation of cracks in components and structures can result in catastrophic failure. Therefore, early crack identification plays a vital role in the safe operation of plants, machinery and high integrity structures by providing timely damage assessment and, therefore, maintains high performance and reliability for these systems. System identification, which is an important tool in crack identification, has attracted the attention of the scientific community and there has been a lot of research in the last two decades. The presence of a crack in a component or structure leads to a reduction in the stiffness and to an increase in the damping of the component or structure. The reduction in stiffness results in decreases in the natural frequencies and modifications of the mode shapes of the component or structure. Many researchers have used one or more of these characteristics to detect and locate cracks.

Usually, the determination of the dynamic characteristics of cracked structures outlined above, namely: stiffness, damping, natural frequencies (eigenvalues) and mode shapes (eigenvectors), require full experimental modal survey. This requires the excitation of the structure with a known single force or a known pattern of multiple forces and the measurements of the corresponding responses at various locations on the structure. From these input and output measurement, frequency response functions are determined from which the dynamic characteristics are determined using modal analysis techniques. However, there are real structures such as buildings, bridges, large aircraft, ships and submarines for which it is difficult or impractical to provide an external source of known force excitation. For such systems, it is more practical to measure response only.

Identification and location of cracks from response-only (output-only) measurements has received some attention in the past few years. Duan et al. [1] proposed an approach to assemble a proportional flexibility matrix (PFM) from arbitrarily scaled mode shapes and modal frequencies with response-only data. They integrated the proposed PFMs and flexibility-based damage detection methods for damage localizations using response-only data. This method was applied to a seven degrees of freedom (dofs) mass-spring system and a 53-dof truss structure. Parloo et al. [2] used the sensitivity-based damage assessment techniques using response-only data to identify structural damage defined as local changes in mass or stiffness. Then they proposed another method which is based on the interpretation of shifts in natural frequencies between a reference (undamaged) and a damaged condition [3]. Both of these two methods require the natural frequencies of the structure in its reference and damaged conditions as well as the normalized mode shape estimates from the structure in its reference condition [3]. Lu and Gao [4] presented a new method for damage diagnosis using time-series analysis of vibration signals. The method is based on linear dynamic equations and is formulated as a novel form of the auto-regressive with exogenous (ARX) model with acceleration response-only signals. Also, the standard deviation of the residual error, which is the difference between the measured signals from any actual state of the system and the predicted signals from the ARX model established from a reference (undamaged) state, was found to be a damage-sensitive feature. A damage localization and severity methodology using time-domain response data was presented by Choi and Stubbs [5] using time-domain response-only data. The measured response data in the time domain is spatially expanded over the structure and the mean strain energy for a specified time interval is obtained for each element of the structure. The mean strain energy for each element is, in turn, used to build a damage index that represented the ratio of the stiffness parameter of the pre-damaged (undamaged) to post-damaged (damaged) structure. The damage indices were used to identify possible locations and corresponding severities of damage in the structure.

All the response-only methods in Refs. [2–5] need the parameter of the undamaged state of the structures. However, most suspected damaged civil structures were constructed several decades ago, and the parameter of the structures in the intact state is not available. This is the shortcoming of the existing response-only methods in Refs. [2–5] for damage detection. The method proposed in Ref. [1] is limited by the computational complexity which makes it unusable for real-time online health monitoring of structures. Also, there are errors associated with the fast Fourier transform (FFT) of the measured time data into the frequency domain. The method proposed in this paper overcomes these difficulties.

The identification of cracks based on measured vibration frequencies has been investigated by many authors [6–10]. Narkis [6] reported that the variation of the first two natural frequencies is sufficient for identification of the crack location of a cracked simply supported uniform beam. A damage location assurance criterion was

calculated by Messina et al. [7,8] and was used to identify single defect. The approach was later extended to identify multiple damage sites on the basis of changes in the natural frequencies. Salawu [9] presented a more comprehensive survey in which he reviewed the numerous technical literatures available on crack detection based on the change in natural frequencies. Lee and Chung [10] employed the natural frequencies of a one-dimensional beam-type structure to identify the location and size of a crack. In fact, natural frequencies have been a favoured damage indicator because they can be easily measured and are less contaminated by experimental noise. However, the use of natural frequency changes for crack detection has a major drawback which is that significant cracks may cause only small changes in natural frequencies. Such small changes may go undetected due to measurements errors [11], and errors associated with the transformation of measured time history responses of the structures being investigated, to the frequency domain using the FFT procedure. Generally, it would be necessary for a natural frequency to change by about 5% for damage to be detected with confidence [9].

Due to signal leakage effects caused by using a finite number of time samples, the estimate of amplitude, phase and frequency from the FFT of the measured time histories are normally different from the real ones even in the absence of noise. Applying windowing functions to sampled time signal is a common method in frequency spectrum estimation to minimize the effect of leakage. However, theoretically, the maximum relative error of the amplitude estimate will be 36.4%, 18.1% and 36.4%, respectively, even when Rectangle, Hamming and Hanning windows are employed to minimize leakage [12].

The maximum relative error of the frequency estimate will be $\pm 0.5\Delta f$, where Δf is frequency resolution which is equal to sampling rate divided by the number of points of the FFT. Also, the maximum relative error of the phase estimate will be $\pm 90^\circ$ regardless of the windowing function used [12]. To obtain high-accuracy estimates, several techniques have been proposed to overcome the leakage problem. Huang [13] analysed a windowed signal with Fourier transform and investigated the leakage-induced phase error. He presented an approach to correct leakage in a discrete frequency signal to obtain accurate phase information. Ding and Xie [14] used a three-point convolution correction method to get accurate amplitude of the spectrum. Ming and Kang [15] proposed a new method based on the barycentre of spectral lines in the main lobe to correct the spectral peak value of the spectrum. A new method, based on phase difference between the corresponding discrete spectral lines of the frequency spectrum of two continuous time-domain signals, was proposed by Kang et al. [16].

A comparative study of three existing phase difference correction methods on discrete spectrum was carried out by Ding et al. [17], and the phase difference method proposed in Ref. [16] was recommended for engineering applications. Also, a universal correction formula of frequency, amplitude and phase, based on phase difference of discrete spectrum was investigated by Ding and Zhong [18]. This formula is much more robust than the three-point convolution correction method for a discrete spectrum in Ref. [14] which can only correct the amplitude but is unable to correct frequency and phase. Ding and Jiang [19] found the property that the energy centroid of discrete spectrum of windowing functions used frequently (i.e. Hanning and Rectangular windows, etc.), is near the origin of coordinate. Therefore they proposed a new correction method based on energy centrobaric correction method (ECCM) to get high-accuracy estimate of frequency, phase and amplitude. Zhu et al. [20] employed Parseval's theorem and derived two equalities regarding the line spectrum. Based on this, they proposed a new approach for amplitude correction using the average of multiple points in discrete Fourier transform sequence.

There are the following five novelties associated with the proposed method in this paper, namely: (1) a response-only (output only) damaged state method. It only uses the response time history of damaged beam-like structures and does not need the parameter of the undamaged state of the structures (unlike the other response-only methods in Refs. [2–5]). Also, this method has low computational cost (unlike the response-only method in Ref. [1]) and high precision, and it is, therefore, suitable for online health monitoring of beam-like structures. (2) Moving auxiliary mass for spatial probing of the dynamics of a damaged beam. The natural frequencies of a damaged beam with a traversing auxiliary mass change due to the spatial location of the auxiliary mass along the beam. That is, the auxiliary mass can be used to probe the dynamic characteristics of the beam by traversing the mass from one end of the beam to the other. In real applications, for example in the assessment of a damaged bridge, a motor vehicle can be used as a moving mass and as a vibration exciter. (3) Applications of a spectral centre correction method (SCCM) for correction of frequency spectrum

obtained from the FFT of the response-only time data. SCCM is identical to ECCM which is a practical and effective method used currently in rotating mechanical fault diagnosis, which overcomes the shortcoming of FFT and can provide highly accurate estimates of frequency, amplitude and phase. This is the first paper to apply the ECCM in the field of damage detection of beam-like structures. In this paper, the appellation SCCM is preferred to ECCM as it is more descriptive of the spectral correction as will become apparent subsequently. (4) Use of the derivatives of natural frequency curve for crack identification. Some researches used derivatives of mode shapes as the damage indicator [22,23]. However, natural frequencies have been an appealing damage indicator because they can be easily measured and are less contaminated by experimental noise than mode shapes [11]. Therefore, it is proposed in this paper to use the derivatives of natural frequency curves to provide fast and accurate crack indicator instead of the derivatives of mode shapes which are more contaminated by noise. (5) The use of very basic testing instrumentation. Only a motion sensor, preferably a wireless sensor, connected to a Laptop-based data acquisition system is required for diagnostic tests on a large structure such as a bridge. The excitation and moving mass on the bridge is due to a vehicle driven along the bridge.

It should be noted here that the proposed method for crack identification uses the derivatives of natural frequency curves of beam-like structure with a traversing auxiliary mass. This method, in fact, is an application in structural damage detection of the derivatives (sometimes called 'sensitivities') of eigenvalues with respect to design parameters (or updating parameters). Methods for computing the derivatives of eigenvalues and eigenvectors have been studied by many researchers in the past 30 years [24–32]. The importance of obtaining sensitivities for eigenvalue problems stems from the fact that partial derivatives with respect to design parameters are extremely important for efficient design modifications under given situations, for gaining insight into the reasons for discrepancies between structural analyses and dynamic tests due to design parameters change, and for indicating system model changes that will improve correlations between analyses and tests [31].

For undamped structural eigenvalue problem, expressions were derived for the first derivatives of the eigenvalues by Wittrick [24]. Fox and Kapoor [25] derived expressions for rates of change of eigenvalues and eigenvector to facilitate computerized design of complex structures. Friswell [27] extended Nelson's method [26] for the calculation of the first-order eigenvector derivatives, or sensitivities, to the second- and higher-order eigenvector derivatives. Friswell and Mottershead [28] integrated the works by Wittrick [24], Fox and Kapoor [25], and Nelson [26] in the calculation of sensitivities. A simultaneous interaction scheme of Andrew [29] was analysed and extended, and developed into an effective algorithm for numerical computations of partial derivatives of several eigenvalues and eigenvectors of a matrix which depends on a number of parameters [30]. Adhikari [31] presented rates of change of eigenvalues and eigenvectors of a damped linear discrete dynamic system with respect to the system parameters. The usefulness of the derived expressions was demonstrated by considering an example of non-proportionally damped two-dof system. Choi et al. [32] presented a simple algorithm for the calculation of first-, second- and higher-order derivatives of eigenvalues and eigenvectors of a damped system with repeated eigenvalues. The proposed method found derivatives of eigenvalues and eigenvectors simultaneously from one augmented equation by solving a stable linear algebraic equation.

The design parameters (or updating parameters) with respect to which the derivatives of eigenvalues and eigenvectors have been investigated in the literature include the root diameter of a cylindrical cantilever beam [25], the mean diameter of each tubular members of a pin-connected planar frame [25], the stiffness, breadth and depth of a right angled beam joint [28], the damping of a two-dof system [31], the width of a proportionally damped cantilever beam [32], and the spring stiffness of a five-dof non-proportionally damped mechanical system [32], etc. In this paper, the updating parameter of a beam with an auxiliary mass is the location of the mass along the beam. This kind of updating parameter cannot be found in any literature that have been published. The derivatives of eigenvalues (frequencies) with respect to the locations of an auxiliary mass along a beam have been investigated in this paper for beam-like structure damage detection.

In this paper, the response time histories of damaged simply supported beams with traversing auxiliary mass are computed at various points along its length using the finite element method (FEM). The SCCM is used to calculate highly accurate natural frequencies of the beams with auxiliary mass. The graphical plots of the natural frequencies calculated by SCCM versus axial location of the auxiliary mass are obtained. However, it

is difficult to locate the crack directly from the curves of natural frequencies. A simple and fast method, which is based on the derivatives of the curves of natural frequencies, is proposed. The method provides characteristics which enable detection in beam-like structures. The efficiency and practicability of the proposed method is illustrated via numerical simulation. For real cases, experimental noise is expected to corrupt the response data and, hence, the natural frequencies of the beams. Therefore, response data with a normally distributed random noise is also investigated. Also, the effects of crack depth, auxiliary mass and damping ratios on the proposed method are investigated. From the simulated results, the efficiency and robustness of the proposed method is demonstrated. The proposed method has low computational cost and high precision. Therefore, it has great potential in crack detection of beam-like structures.

2. Auxiliary mass spatial probing

In Ref. [9], it stated that it would be necessary for a natural frequency to change by about 5% for damage to be detected with confidence. Also, the authors of this paper found by using finite element analysis that for a damaged simply supported beam without an auxiliary mass, the natural frequency change (comparing with the frequency of an intact beam) is about 5.0% for the first mode of bending vibration when the crack ratio is greater than 50%. That is, a crack whose crack ratio, which is the ratio of the depth of the crack to the depth of the beam, is greater than 50% can be detected with confidence using the natural frequency change of a structure. Therefore, it is difficult to make damage detection directly using the natural frequencies of a damaged beam itself. In the paper, an auxiliary mass is added to a damaged beam to magnify the crack effect and, hence, to facilitate damage detection of the beam. The detail of this approach is described as follows.

A simply supported beam carrying an auxiliary mass with a single-sided transverse crack whose depth is H_c, is shown in Fig. 1. The crack is located at position $x = l_c$ from the left support of the beam. The width, depth and length of the beam are, respectively, B, H and L, while m is the auxiliary mass which is located at position $x = l_m$.

The natural frequencies of a damaged beam with a traversing auxiliary mass change due to the spatial location of the auxiliary mass along the beam. This is because the flexibility and inertia of the beam depend on the axial location of the auxiliary mass. Therefore the auxiliary mass can amplify crack effects, especially when located close to a crack. That is, the auxiliary mass can be used to probe the dynamic characteristics of the beam by traversing the mass from one end of the beam to the other.

As shown in Fig. 2, the first two natural frequency curves of a cracked beam with an auxiliary mass traversing along the length of the beam are single smooth curves. The beam has a cross-sectional area of $0.100 \times 0.025\,\mathrm{m}^2$ and its length is 2.4 m. A crack of depth $h_c = 2.5$ mm is located at $l_c = 0.4$ m. Hence, it is hard to detect cracks in simply supported beams by using data directly from the graphical plot of natural frequency versus axial location of auxiliary mass. The object of this work is to propose a simple approach based on the derivatives of the curve of the corrected high-accuracy natural frequencies, to provide characteristics which will enable detection in beam-like structures.

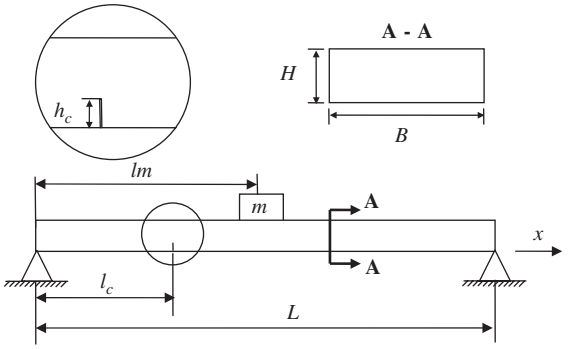

Fig. 1. Model of a cracked simply supported beam with auxiliary mass.

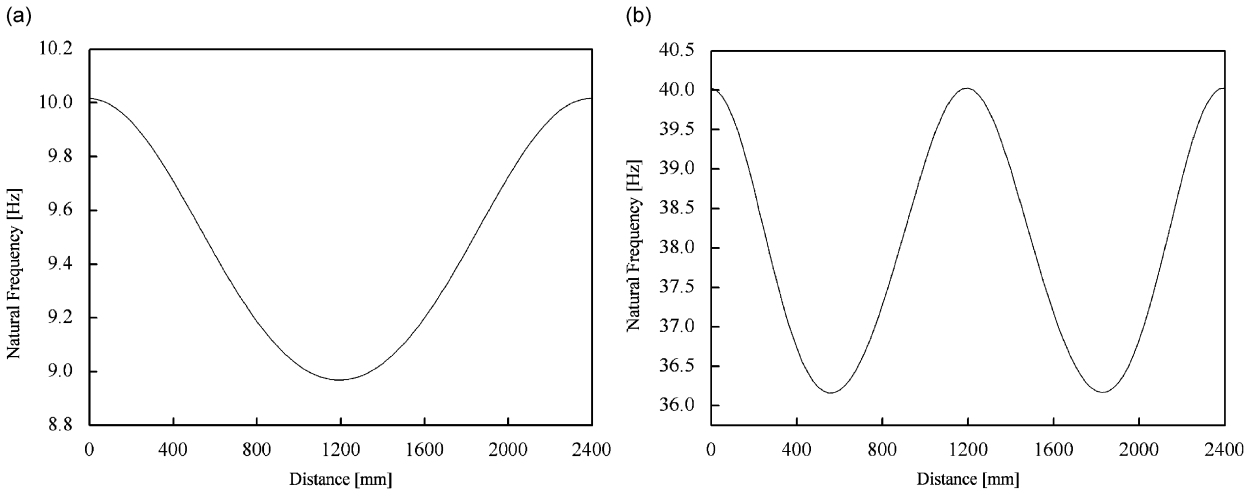

Fig. 2. The first two natural frequency curves of the cracked aluminium alloy beam ($L = 2.4$ m, $H = 25$ mm, $B = 100$ mm, $h_c = 2.5$ mm, $l_c = 0.4$ m, beam mass $m_b = 16.2$ kg) with an auxiliary mass traversing along the beam ($m = 2$ kg): (a) first natural frequency curve and (b) second natural frequency curve.

3. Spectral centre correction method

3.1. Shortcoming of FFT

Due to the spectrum leakage effect caused by a finite number of processed samples, the estimated frequency spectrum resulting from the FFT of the response time data is normally different from the actual spectrum even in the absence of noise. For instance, as mentioned in the Introduction, the maximum relative error of the amplitude estimate will be 36.4%, 18.1% and 36.4%, respectively, even when Rectangle, Hamming and Hanning windows are employed in order to minimize leakage [12]. The maximum relative error of the frequency estimate will be $\pm 0.5\Delta f$, where Δf is the frequency resolution which is equal to the sampling rate divided by the number of points of the FFT. Also, the maximum relative error of the phase estimate will be $\pm 90^\circ$ regardless of the windowing function used [12]. It is well known that there is no spectral leakage in the FFT of a finite synchronously sampled periodic signal sequence, in which an integer multiple of periods is measured. Unfortunately, in practical situations, it is often difficult for the sampling procedure to be exactly synchronized with periodic signals [33]. SCCM is a very accurate and reliable method to obtain high-accuracy estimates of frequency, phase and amplitude of the signals.

Furthermore, in spectrum analysis, the spectral lines of the frequency spectrum obtained from the FFT of the response time history is discrete, as shown in Fig. 3. The spectral lines are the re-sampled results of the complex convolution of the signal spectrum and the window function spectrum with the equal frequency interval of Δf. If the frequency of the signal coincides with a spectral line, the frequency, amplitude and phase angle of the signal are accurate. However, in real applications, the frequency of the signal usually lies between two spectral lines and does not overlap the spectrum peak (i.e. point A in Fig. 3). Therefore, the frequency, amplitude and phase angle of the signal are not accurate. For example, the error of the frequency of the main spectral line shown in Fig. 3 is f_e, while the error of the corresponding spectral amplitude is A_e.

3.2. Theory of SCCM

This section presents a brief background on the SCCM utilized in this paper. The SCCM is identical to the ECCM proposed by Ding et al. [19,21]. More facts may be found in Refs. [19,21] which are not readily accessible as they are written in Chinese. It should be noted that this paper is the first presentation of the ECCM in English. In this paper, the method is referred to as SCCM as it is more descriptive of the techniques.

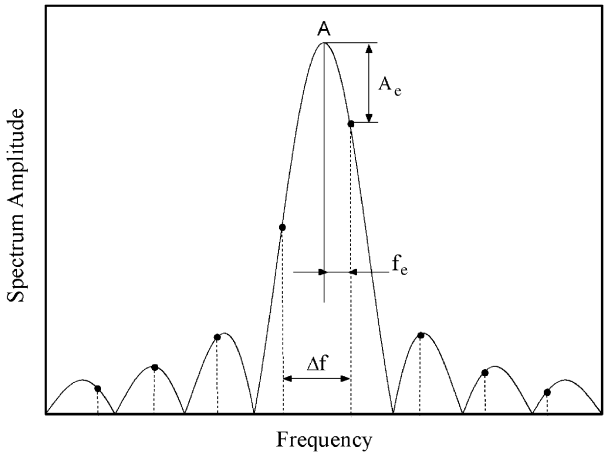

Fig. 3. Discrete spectral lines re-sampled in frequency domain.

The term ECCM is a direct translation of the name of the method in Mandarin. The energy property of the power spectrum of the Hanning window is discussed as follows. For a time history data set of size N, the Hanning window is defined as [15]

$$W(n) = 0.5 - 0.5\cos(2\pi n/N), \tag{1}$$

where $n = 0,1,2,\ldots, N-1$ and $W(n)$ is the amplitude of the Hanning window for the nth data. The spectrum function of Hanning window is [15]

$$W(\omega_n) = \left\{ aD(\omega_n) + \frac{1-a}{2}\left[D\left(\omega_n - \frac{2\pi}{N}\right) + D\left(\omega_n + \frac{2\pi}{N}\right)\right]\right\} \mathrm{e}^{-\mathrm{i}(N\omega_n/2)}, \tag{2}$$

where

$$D(\omega_n) = \sin(N\omega_n/2)/\sin(\omega_n/2)\,\mathrm{e}^{\mathrm{i}\omega_n/2}, \tag{3}$$

$$\omega_n = k\,\Delta\omega_n, \tag{4}$$

$$\Delta\omega_n = \frac{2\pi}{N}, \tag{5}$$

$$a = 0.5 \tag{6}$$

and $\Delta\omega_n$ is normalized frequency resolution, k is the spectral line number.

Generally, $N \gg 1$ so that $1/N \to 0$. Therefore,

$$\sin\left(\frac{\omega_n}{2}\right) = \sin\left(\frac{k\pi}{N}\right) \approx \frac{k\pi}{N}. \tag{7}$$

From Eq. (2), the three terms in parentheses have a phase difference of $2\pi/N$. Neglecting the phase difference (because $N \gg 1$) and referring to Eq. (7), the main lobe function (modulus function) M_f of Hanning window, which is the sum of the modulus function of these three terms, can be obtained as

$$\begin{aligned} M_f &= a\frac{\sin(\pi k)}{\pi k} + \frac{1-a}{2}\left[\frac{\sin\,\pi(k-1)}{\pi(k-1)} + \frac{\sin\,\pi(k+1)}{\pi(k+1)}\right] \\ &= \frac{\sin(\pi k)}{\pi k}\,\frac{a + (1-2a)k^2}{1-k^2}. \end{aligned} \tag{8}$$

When $k=0$, $M_f \to a$. When $k \to \pm 1$, according to L'Hospital's rule, the following limiting value is obtained:

$$\lim_{k\to\pm1} \frac{\sin(\pi k)}{\pi k} \frac{a+(1-2a)k^2}{1-k^2} = \lim_{k\to\pm1} \frac{\{\sin(\pi k)[a+(1-2a)k^2]\}'}{[\pi k(1-k^2)]'} = \frac{1-a}{2}. \tag{9}$$

Therefore, when $k \to \pm 1$, $M_f \to (1-a)/2$. Also, when $k = \pm 2, \pm 4, \ldots$, $M_f = 0$.

When the windowing function is Hanning window, $a = 0.5$. Therefore, the main lobe function (modulus function) M_f of Hanning window is

$$M_f = \frac{\sin(\pi k)}{2\pi k(1-k^2)}. \tag{10}$$

The main lobe function of Hanning window is shown in Fig. 4(a). Eq. (10) and Fig. 4(a) show that the width of the main lobe is equal to the frequency interval between four spectral lines. That is, there exists four spectral lines within the main lobe.

In fact, when $k = 0, \pm 1, \pm 2, \ldots$, the centre of the main lobe coincides with one spectral line. But when the spectral line does not overlap the centre of the main lobe, there are errors in the estimates of the frequency,

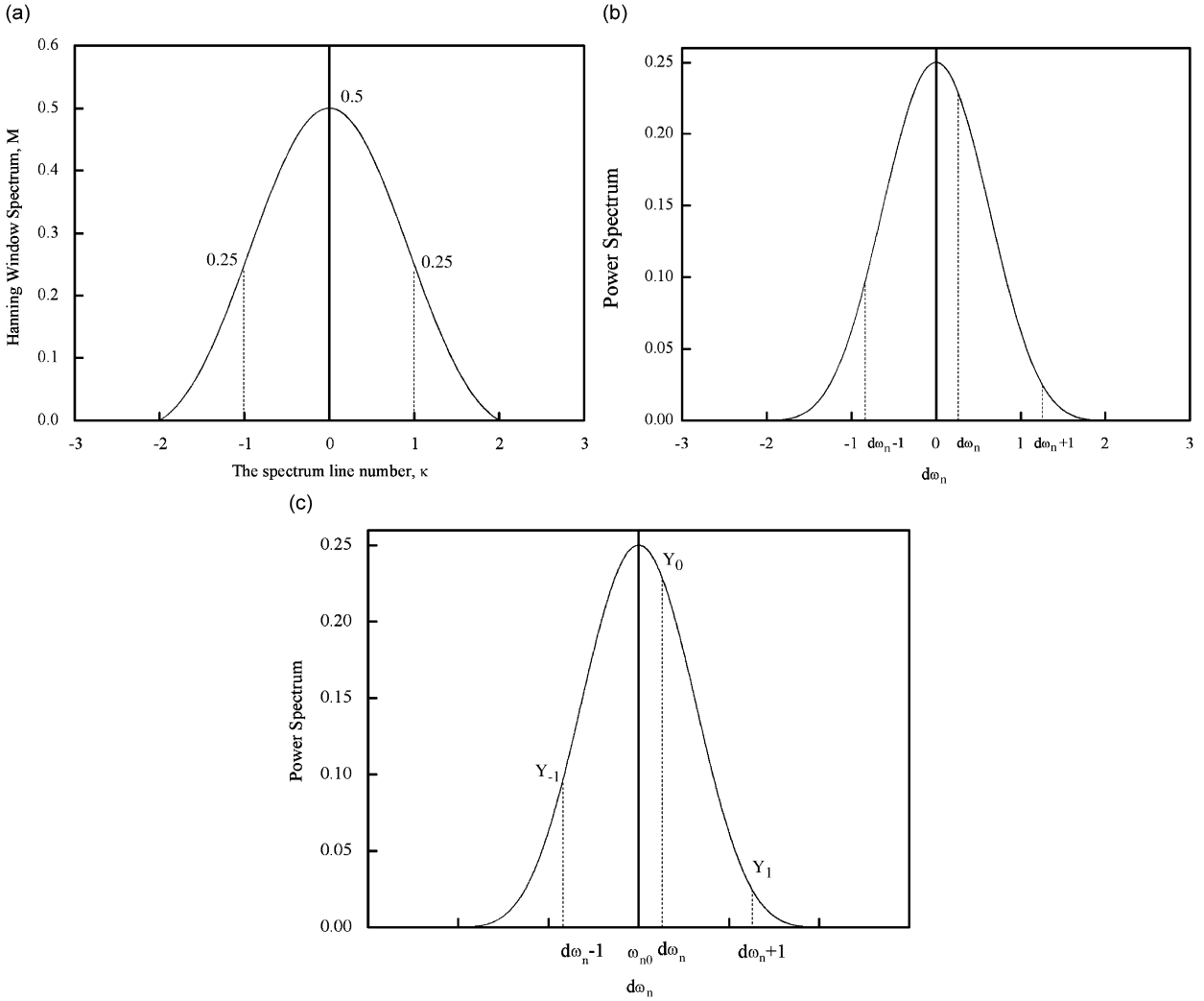

Fig. 4. Hanning window: (a) main lobe function of Hanning window; (b) power spectrum of Hanning window when the centrobaric coordinate of main lobe is zero; and (c) power spectrum of Hanning window when the centrobaric coordinate of main lobe is ω_{n0}.

amplitude and phase angle. The importance of the SCCM is in calculating the centre frequency of the main lobe from the spectral lines resulting from the FFT of the time history. This enables the derivation of accurate estimates of frequency, amplitude and phase angle of the time-domain signal.

For the case that the spectral line does not overlap the centre of the main lobe, k is replaced by $d\omega_n$, and Eq. (10) can be expressed as

$$M_f = \frac{\sin(\pi d\omega_n)}{2\pi d\omega_n(1-d\omega_n^2)}, \tag{11}$$

where $d\omega_n$ is the normalized frequency correction value which is shown in Fig. 4(b).

In fact,

$$\omega_{na} = \omega_n + d\omega_n, \tag{12}$$

where ω_{na} is the accurate normalized frequency of the time-domain signal.

Now, from Eq. (11), the power spectrum of Hanning window can be obtained as

$$G_{wp}(d\omega_n) = \frac{\sin^2(\pi d\omega_n)}{4\pi^2 d\omega_n^2(1-d\omega_n^2)^2}. \tag{13}$$

From Fig. 4(b) and Eq. (13), the power spectrum of Hanning window, for a given value $d\omega_n$ and $n = 0,1,2,\ldots,\infty$, can be obtained as

$$\begin{aligned}
&\sum_{i=-n}^{n} G_{wp}(d\omega_n + i)(d\omega_n + i) \\
&\quad = \sum_{i=-n}^{n} \frac{\sin^2[\pi(d\omega_n + i)]}{4\pi^2(d\omega_n + i)^2[1-(d\omega_n + i)^2]^2}(\omega + i) \\
&\quad = \frac{-\sin^2(\pi d\omega_n)}{16\pi^2(n + d\omega_n)^2(n + d\omega_n + 1)^2} + \frac{\sin^2(\pi d\omega_n)}{16\pi^2(n - d\omega_n)^2(n - d\omega_n + 1)^2}.
\end{aligned} \tag{14}$$

Therefore,

$$\sum_{i=-n}^{n} G_{wp}(d\omega_n + i)(d\omega_n + i) = 0, \tag{15}$$

when $n = \infty$.

Eq. (15) shows that the energy centrobaric of the power spectrum of Hanning window is zero. That is, it approaches the origin of coordinates as the number of spectral lines used to represent the signal approaches infinity.

If the centrobaric coordinate of the main lobe is shifted to ω_{n0} and the power spectrum is multiplied by A, the power spectrum shown in Fig. 4(c) will be

$$Y(\omega) = A\frac{\sin^2[\pi(d\omega_n - \omega_{n0})]}{4\pi^2(d\omega_n - \omega_{n0})^2[1-(d\omega_n - \omega_{n0})^2]^2}, \tag{16}$$

where ω_{n0} and A are, respectively, the normalized frequency and amplitude of the sampled signal. From Eqs. (15) and (16), the following equation can be obtained:

$$\sum_{i=-n}^{n} Y_i(d\omega_n - \omega_{n0} + i) = 0, \tag{17}$$

where Y_0 is the largest peak value of spectral lines and Y_i is the peak value of the ith spectral line. Therefore, the centrobaric coordinate of the main lobe is

$$\omega_{n0} = \frac{\sum_{i=-n}^{n} Y_i(d\omega_n + i)}{\sum_{i=-n}^{n} Y_i}. \tag{18}$$

Eq. (18) is the accurate estimate formula of frequency for single sinusoidal signal when Hanning window is used.

If f_s is sampling rate, N is the number of points of the FFT, m is the number of spectral lines of the discrete spectrum, the accurate estimate of the frequency of the sampled signal, ω_0, can be obtained as

$$\omega_0 = \frac{\sum_{i=-n}^{n} Y_i(m+i)}{\sum_{i=-n}^{n} Y_i} f_s/N. \tag{19}$$

According to Parseval's theorem, namely, that the sum (or integral) of the square of a signal is equal to the sum (or integral) of the square of its transform, the accurate estimate formula of amplitude can be obtained as

$$A = \sqrt{K_t \sum_{i=-n}^{n} Y_i}, \tag{20}$$

where K_t is a coefficient due to the added windowing function, which can be calculated by the following equation:

$$K_t = \frac{\int_0^T x^2(t)\,\mathrm{d}t}{\int_0^T |w(t)x^2(t)|^2\,\mathrm{d}t}, \tag{21}$$

where $x(t)$ and $w(t)$ are, respectively, the analysed signal and the added window.

From Eq. (19), $\Delta\omega$, the frequency correction value, can be expressed as

$$\Delta\omega = (\omega_0 - mf_s/N)/(f_s/N). \tag{22}$$

Therefore, the correction of the phase is [15]

$$\Delta\phi = -\Delta\omega\,\pi. \tag{23}$$

Assuming that the real and imaginary part of the FFT of the signal are, respectively, R_k and I_k, the accurate estimate formula of phase can be obtained as

$$\phi = tg^{-1}\left(\frac{R_k}{I_k}\right) + \Delta\phi. \tag{24}$$

The power spectrum of Hanning window shown in Fig. 4(a) shows only the main lobe; the side lobes are not visible because they are very small. Therefore, in real applications, accurate frequency, amplitude and phase can be calculated by using the few spectral lines which are associated with the main lobe. In fact, only three spectral lines ($n = 1$) need to be used for computing highly accurate estimates of amplitude. This results in the three-point convolution correction method [14]. Theoretically, using more spectral lines will result in a more accurate estimate of frequency, amplitude and phase. However, different frequency components will interfere with each other. Therefore, only few spectral lines need to be used for spectrum correction, the number of spectral lines depends on how close the frequency components are, the degree of accuracy of the correction desired, and the desired speed of the computation.

3.3. Numerical evaluation of SCCM

In order to illustrate spectral correction using the SCCM, the following multi-frequency signal was used to generate time data:

$$y(t) = \cos(2\pi f_1 t + \phi_1) + \cos(2\pi f_2 t + \phi_2) + \cos(2\pi f_3 t + \phi_3) + \cos(2\pi f_4 t + \phi_4) + r(t), \tag{25}$$

where $[f_1\ f_2\ f_3\ f_4]^t = [10.3\ 40.5\ 87.6\ 148.2]^t$, $[\phi_1\ \ \phi_2\ \ \phi_3\ \ \phi_4]^t = \pi/180[10\ \ 20\ \ 30\ \ 40]^t$ and $r(t)$ was a normally distributed random noise. Eq. (25) represented a complex periodic signal which consists of four sinusoidal components of frequencies 10.3, 40.5, 87.6, and 148.2 Hz. These frequencies were chosen to ensure that they do not coincide with the spectral frequencies obtained from the FFT of the signal. The corresponding phase angles of the four sinusoidal components of the complex periodic signal are: 10°, 20°, 30°, and 40°. Using a sampling rate of 1000 Hz, four data sets consisting of 512, 1024, 2048 and 4096 data points were generated from Eq. (25). By means of the FFT procedure and the Hanning window, four frequency spectrums were

produced from the four time-domain data sets. Then, the SCCM was applied to the frequency spectrums in order to obtain accurate estimates of the frequencies. Table 1 shows a comparison of frequencies calculated by FFT and SCCM when $n = 5$. That is, 11 spectral lines were used for frequency estimate. Two different levels of noise (0% and 20% of amplitude of the signal) were investigated. It is noted here that the normally distributed random noise whose amplitude is 0% or 20% of the amplitude of the noise-free time data is added to the noise-free time data. From Table 1, it is seen that the results of frequency correction are highly accurate even if additive noise is as high as 20%. Taking the frequency component 10.3 Hz as an example, when a noise of 20% was added and the number of processed time data points is 512, the frequency calculated by FFT is 9.765625 Hz and its relative error is −51.88107‰, whereas, the frequency calculated by SCCM is 10.300045 Hz and its relative error is 0.00437‰ (where ‰ denotes per 1000). When the number of processed time data is 4096, the relative error of the frequency component 10.3 Hz calculated by FFT is −0.447515%, whereas, that of the frequency component 10.3 Hz calculated by SCCM is 0.004709%. An error of 0.4% in the frequency estimation by FFT is very significant in structural damage detection, especially, for small crack detection. Taking an example, the authors found that for a damaged simply supported beam, the natural frequency

Table 1
Comparison of frequencies calculated by FFT and SCCM, in which Hanning window was used, sampling rate is 1000 Hz, number of processed time data is N, and 11 spectral lines are used ($n = 5$)

	Simulation frequency		FFT result		SCCM result	
	Noise (%)	Value (Hz)	Value (Hz)	Relative error (‰)	Value (Hz)	Relative error (‰)
$N = 512$	0	10.300000	9.765625	−51.881068	10.300045	0.004369
		40.500000	41.015625	12.731481	40.500005	0.000123
		87.600000	87.890625	3.317637	87.599996	−0.000046
		148.20000	148.43750	1.602564	148.20000	−0.000007
	20	10.300000	9.765625	−51.881068	10.311881	1.153495
		40.500000	41.015625	12.731481	40.489574	−0.257432
		87.600000	87.890625	3.317637	87.599945	−0.000628
		148.20000	148.43750	1.602564	148.20206	0.013920
$N = 1024$	0	10.300000	10.742188	42.930874	10.300010	0.000971
		40.500000	40.039063	−11.381160	40.499986	−0.000346
		87.600000	87.890625	3.317637	87.600005	0.000057
		148.20000	148.43750	1.602564	148.20000	0.000020
	20	10.300000	10.742188	42.930874	10.298328	−0.162330
		40.500000	40.039063	−11.381160	40.497920	−0.051358
		87.600000	87.890625	3.317637	87.599169	−0.009486
		148.20000	148.43750	1.602564	148.20010	0.000648
$N = 2048$	0	10.300000	10.253906	−4.475146	10.299999	−0.000097
		40.500000	40.527344	0.675160	40.500000	0.000000
		87.600000	87.402344	−2.256347	87.599995	−0.000057
		148.20000	148.43750	1.602564	148.20000	0.000047
	20	10.300000	10.253906	−4.475146	10.298970	−0.100000
		40.500000	40.527344	0.675160	40.499235	−0.018889
		87.600000	87.402344	−2.256347	87.599467	−0.006084
		148.20000	148.43750	1.602564	148.19864	−0.009150
$N = 4096$	0	10.300000	10.253906	−4.475146	10.300000	0.000000
		40.500000	40.527344	0.675160	40.500000	0.000000
		87.600000	87.646484	0.530639	87.600000	0.000000
		148.20000	148.19336	−0.044811	148.200000	0.000000
	20	10.300000	10.253906	−4.475146	10.300485	0.047087
		40.500000	40.527344	0.675160	40.500279	0.006889
		87.600000	87.646484	0.530639	87.599740	−0.002968
		148.20000	148.19336	−0.044811	148.20071	0.004811

Note: % denotes per 100, ‰ denotes per 1000.

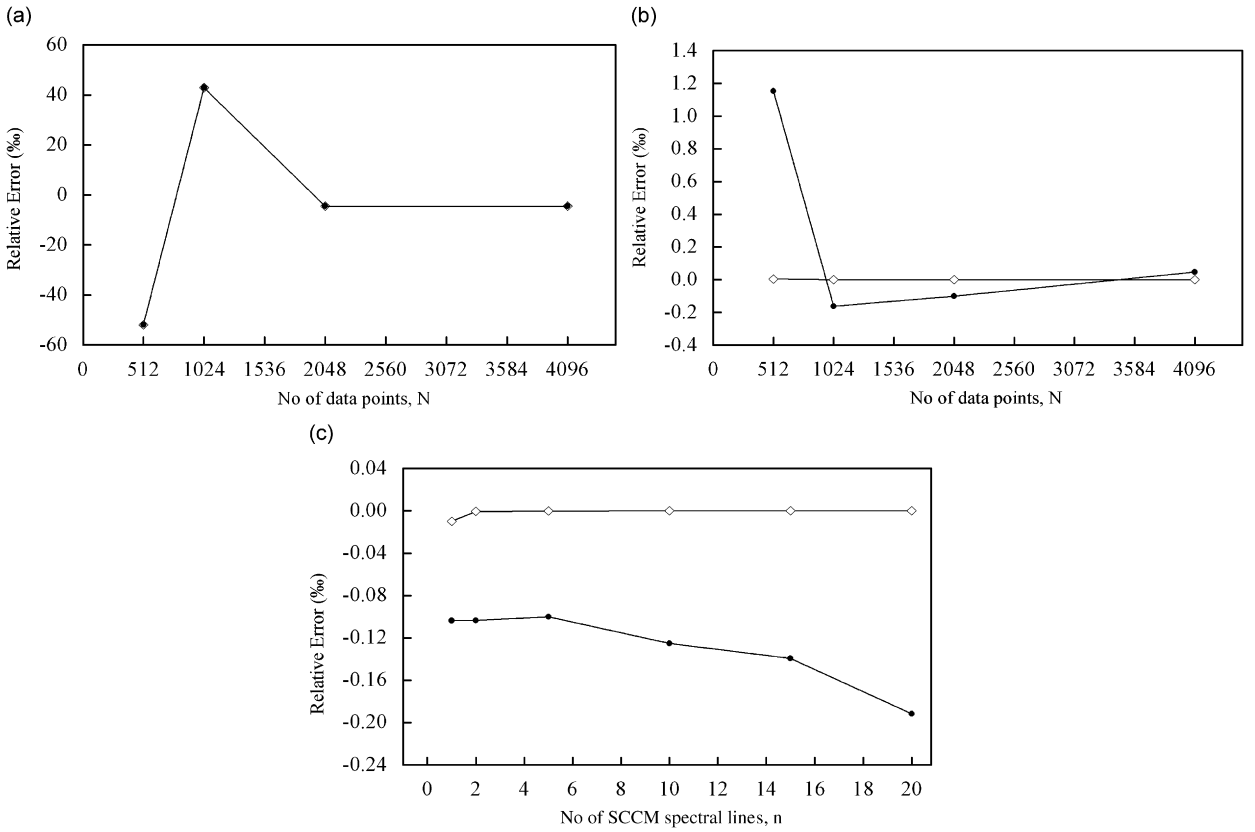

Fig. 5. Comparisons of the relative errors of frequency estimate by FFT and SCCM using different data points and spectral lines: (a) error using different number of data points (FFT); (b) error using different number of data points (SCCM); and (c) error using different SCCM spectral lines: (—◇—) no noise and (—●—) 20% noise. (*Note*: For FFT, relative error is the same with or without added noise.)

change (comparing with the frequency of an intact beam) is about 0.4% for the first mode of bending vibration when the crack ratio is 30%. Therefore, high accuracy frequency estimation by SCCM has great potential in the field of structural damage detection. Figs. 5(a) and (b) show the relation between the relative errors and the number of processed time data points. It can be seen from Table 1 and Figs. 5(a) and (b) that the accuracy of frequency estimate increases when the number of points increases.

The relation between spectral lines used for frequency estimate and the accuracy of frequency estimate was investigated. Figs. 5(c) show the relation between the relative errors and the number of spectral lines used. Table 2 shows the results obtained using different spectral lines ($n = 1, 2, 5, 15$) in the SCCM procedure. From the table, it can be deduced that the accuracy of frequency estimate increases when the spectral lines N_s increase from 3 to 11, that is, n increases from 1 to 5 since $N_s = 2n+1$. However, it can be seen from Fig. 5(c), when spectral lines increase from 21 ($n = 10$), to 31 ($n = 15$) and to 41 ($n = 20$), the accuracy of frequency estimates decreases. The reason is that the frequency components will couple when more spectral lines are used.

3.4. Evaluation of SCCM in beam-like structures

In this section, a simply supported beam with auxiliary mass located at various axial positions is studied using the ABAQUS finite element code. The beam models are made of aluminium of cross-sectional area $100 \times 25\,\text{mm}^2$ with a length of 2400 mm. Finite elements of type 20node 3D brick elements, which are denoted in the ABAQUS FE package as C3D20R, are used. The beam models have the following material properties: Young's modulus $E = 70\,\text{GPa}$, Density $\rho = 2700\,\text{kg/m}^3$, Poisson ratio $v = 0.34$. Two sets of data are

Table 2
Comparison of frequencies calculated by FFT and SCCM, in which Hanning window was used, sampling rate is 1000 Hz, number of processed time data is 2048, and different spectral lines are used ($n = 1, 2, 5, 15$)

	Simulation frequency		FFT result		SCCM result	
	Noise (%)	Value (Hz)	Value (Hz)	Relative error (‰)	Value (Hz)	Relative error (‰)
$n = 1$	0	10.300000	10.253906	−4.475146	10.299898	−0.009903
		40.500000	40.527344	0.675160	40.500021	0.000519
		87.600000	87.402344	−2.256347	87.592222	−0.088790
		148.20000	148.43750	1.602564	148.21326	0.089494
	20	10.300000	10.253906	−4.475146	10.298932	−0.103689
		40.500000	40.527344	0.675160	40.499217	−0.019333
		87.600000	87.402344	−2.256347	87.591729	−0.094418
		148.20000	148.43750	1.602564	148.21209	0.081559
$n = 2$	0	10.300000	10.253906	−4.475146	10.299994	−0.000583
		40.5000000	40.527344	0.675160	40.500001	0.000025
		87.600000	87.402344	−2.256347	87.599673	−0.003733
		148.20000	148.43750	1.602564	148.20046	0.003097
	20	10.300000	10.253906	−4.475146	10.298934	−0.103495
		40.500000	40.527344	0.675160	40.499227	−0.019086
		87.600000	87.402344	−2.256347	87.599240	−0.008676
		148.20000	148.43750	1.602564	148.19864	−0.009184
$n = 5$	0	10.300000	10.253906	−4.475146	10.299999	−0.000097
		40.500000	40.527344	0.675160	40.500000	0.000000
		87.600000	87.402344	−2.256347	87.599995	−0.000057
		148.20000	148.43750	1.602564	148.20000	0.000047
	20	10.300000	10.253906	−4.475146	10.298970	−0.100000
		40.500000	40.527344	0.675160	40.499235	−0.018889
		87.600000	87.402344	−2.256347	87.599467	−0.006084
		148.20000	148.43750	1.602564	148.19864	−0.009150
$n = 15$	0	10.300000	10.253906	−4.475146	10.300000	0.000000
		40.500000	40.527344	0.675160	40.500000	0.000000
		87.600000	87.402344	−2.256347	87.600000	0.000000
		148.20000	148.43750	1.602564	148.20000	0.000000
	20	10.300000	10.253906	−4.475146	10.298565	−0.139320
		40.500000	40.527344	0.675160	40.498712	−0.031802
		87.600000	87.402344	−2.256347	87.599342	−0.007511
		148.20000	148.43750	1.602564	148.19813	−0.012611

Note: % denotes per 100, ‰ denotes per 1000.

calculated by ABAQUS as follows: firstly, the natural frequencies of the intact beam with the traversing auxiliary mass are computed by performing eigenvalue extraction; secondly, dynamic time history responses of the simply supported beam with mass are obtained by using modal superposition. In the second step, the input force, shown in Fig. 6(a), is applied to the intact beam at the position of 7/24th of its length from one end. The input force used was a chirp signal generated by the Matlab programming software. The frequency of the signal starts at 0 Hz and ends at 250 Hz. The chirp signal has a duration of 2.048 s and a peak-amplitude of 10 N. The response data, which is shown in Fig. 6(b), is obtained at the position of 13/24th of the length of the intact beam. Then the time-domain dynamic response data computed by the ABAQUS FEA software was transformed into the frequency domain using the FFT and SCCM procedures. Thus the natural frequencies of the simply supported beam with an auxiliary mass can be obtained.

Fig. 7 shows the frequency spectrum obtained using the FFT procedure. It is seen that the natural or modal frequencies of the intact beam change if the auxiliary mass is located at different positions along the length of the beam. When the mass is located at the end of the beam (i.e. $l_m = 0$), Fig. 7 and Table 3 show that the natural frequencies are identical to those of an intact beam because the mass has no dynamic effect. When the

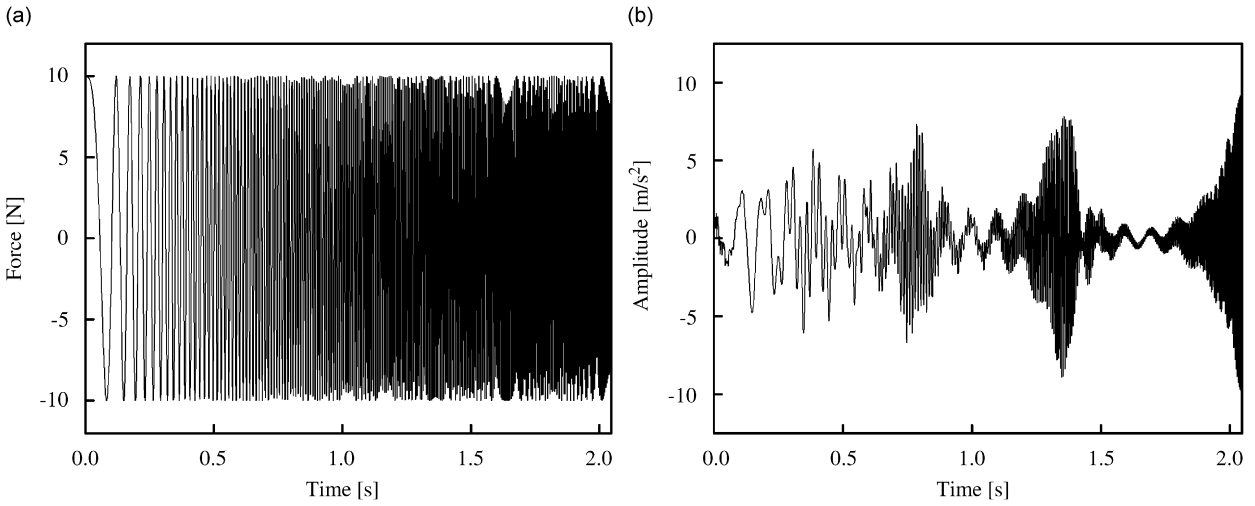

Fig. 6. (a) Force input data and (b) response time data of an intact simply supported beam with an auxiliary mass.

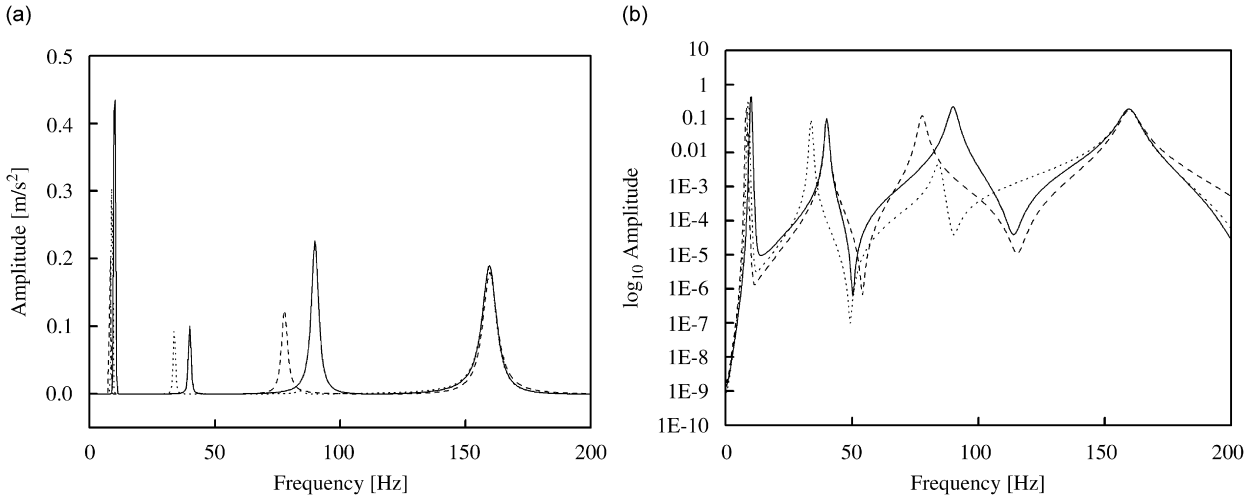

Fig. 7. Frequency spectrum of time history of an intact aluminium beam ($\zeta = 0.02$) with an auxiliary mass ($m = 4$ kg) located at different positions (l_m) of the beam, (a) linear vertical coordinate, and (b) logarithmic vertical coordinate: (——) $l_m = 0$ m, (· · · · · ·) $l_m = 0.6$ m, and (– – – –) $l_m = 1.2$ m.

Table 3
Natural frequencies of intact beam with and without auxiliary mass

Auxiliary mass (kg)	Location, l_m (m)	Frequency (Hz)			
		First mode	Second mode	Third mode	Fourth mode
0	–	10.2539	40.0390	89.8438	159.6680
4	0	10.2539	40.0390	89.8438	159.6680
4	0.6	8.7890	33.6914	83.9844	159.6680
4	1.2	8.3007	40.0390	77.6367	159.6680

mass is located at the centre of the beam (i.e. $l_m = 1.2$ m), Fig. 7 and Table 3 show that the natural frequencies of the odd modes (modes 1 and 3) are less than those of the intact beam without auxiliary mass or with the mass located at the end of the beam ($l_m = 0$). But the natural frequencies of the even modes (modes 2 and 4) are practically the same as those of the intact beam without auxiliary mass or with auxiliary mass at $l_m = 0$. This difference is due to the fact that the centre of the beam is an antinodal position for the odd modes but a nodal position for the even modes.

Thus, when the mass is located at the centre, the dynamics of the odd modes of the beam are significantly affected whereas the dynamics of the even modes are hardly affected. But when the mass is located at $l_m = 0.6$ m, which is 1/4 length of the beam, only modes which are multiples of 4 will have nodes at the same location. The frequencies of these modes will be least affected. But the frequencies of all other modes will be significantly affected as seen in Fig. 7 and Table 3. Thus, from these results, it is very clear that the natural frequencies of a beam with an auxiliary mass are significantly affected by the location of the mass. Therefore, the auxiliary mass can be used to probe the dynamic characteristics of the beam by traversing the mass from one end of the beam to the other. The accuracy of the frequency is the major factor when the frequency change is used for crack indication. But as stated previously, the frequency estimates obtained from the FFT procedure are not very accurate. The use of the SCCM approach provides more accurate estimates of frequencies.

In order to evaluate the effect of damping ratios on the estimate of the resonance frequencies of beam-like structures, beams with different damping ratios were also investigated. Fig. 8 shows the frequency spectrum of response data of an intact beam with different damping ratios. It is seen that the peak response amplitudes reduce as the damping is increased. But the change in magnitude of the amplitude is greater than the change in magnitude of the damping. For example, when the damping ratio ζ increases from 0.02 to 0.05, that is an increase by a factor of 2.5, the amplitude of mode 3 is reduced by a factor of 8. The effect of damping on the resonance frequencies is discussed separately in Section 4.4.

The three sets of natural frequencies curves for mode 1 computed for the three damping ratios ($\zeta = 0.02$, 0.05, and 0.10) using FE eigenvalue extraction, FFT of response data and SCCM of response data, are plotted against the corresponding axial locations of the auxiliary mass as shown in Fig. 9(a-1)–(a-3), respectively. As can be seen from these figures, the precision of frequencies calculated by FFT of response data of the beam is low, whereas, the frequencies calculated by SCCM of FFT of response data are very accurate. The corresponding relative errors between the frequencies calculated by SCCM and FFT are shown in Fig. 9(b-1)–(b-3) for the three different damping ratios ($\zeta = 0.02$, 0.05, and 0.10). From Fig. 9(b-1)–(b-3), it seen that the relative error of frequencies calculated by SCCM increases when the damping ratio increases.

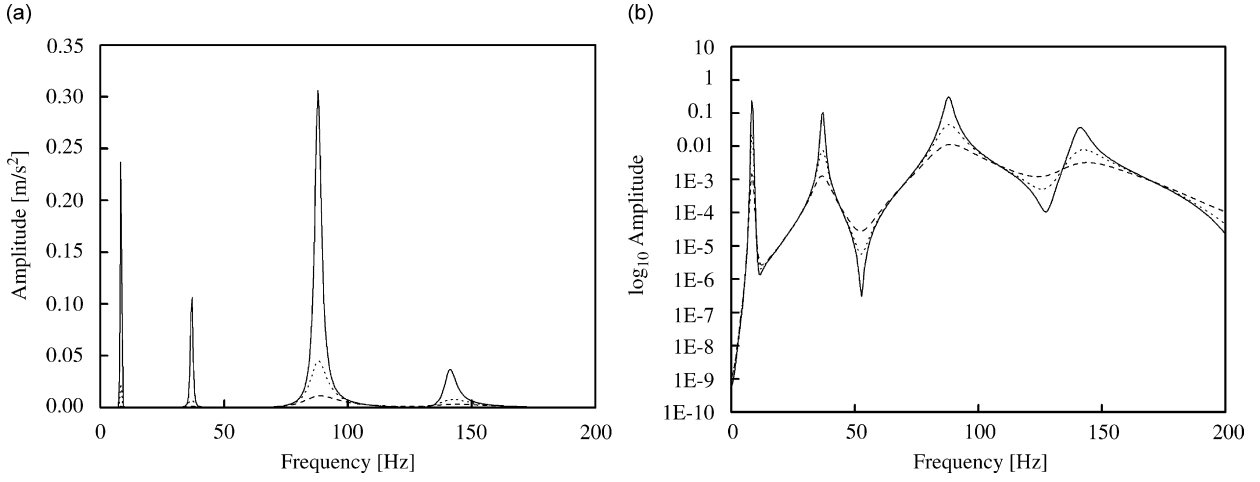

Fig. 8. Frequency spectrum of time history of an intact aluminium beam with an auxiliary mass ($m = 4$ kg) located at position of $l_m = 0.9$ m of the beam for varying damping ratios, (a) linear vertical coordinate, and (b) logarithmic vertical coordinate: (——) $\zeta = 0.02$, (· · · · ·) $\zeta = 0.05$ and (– – – –) $\zeta = 0.10$.

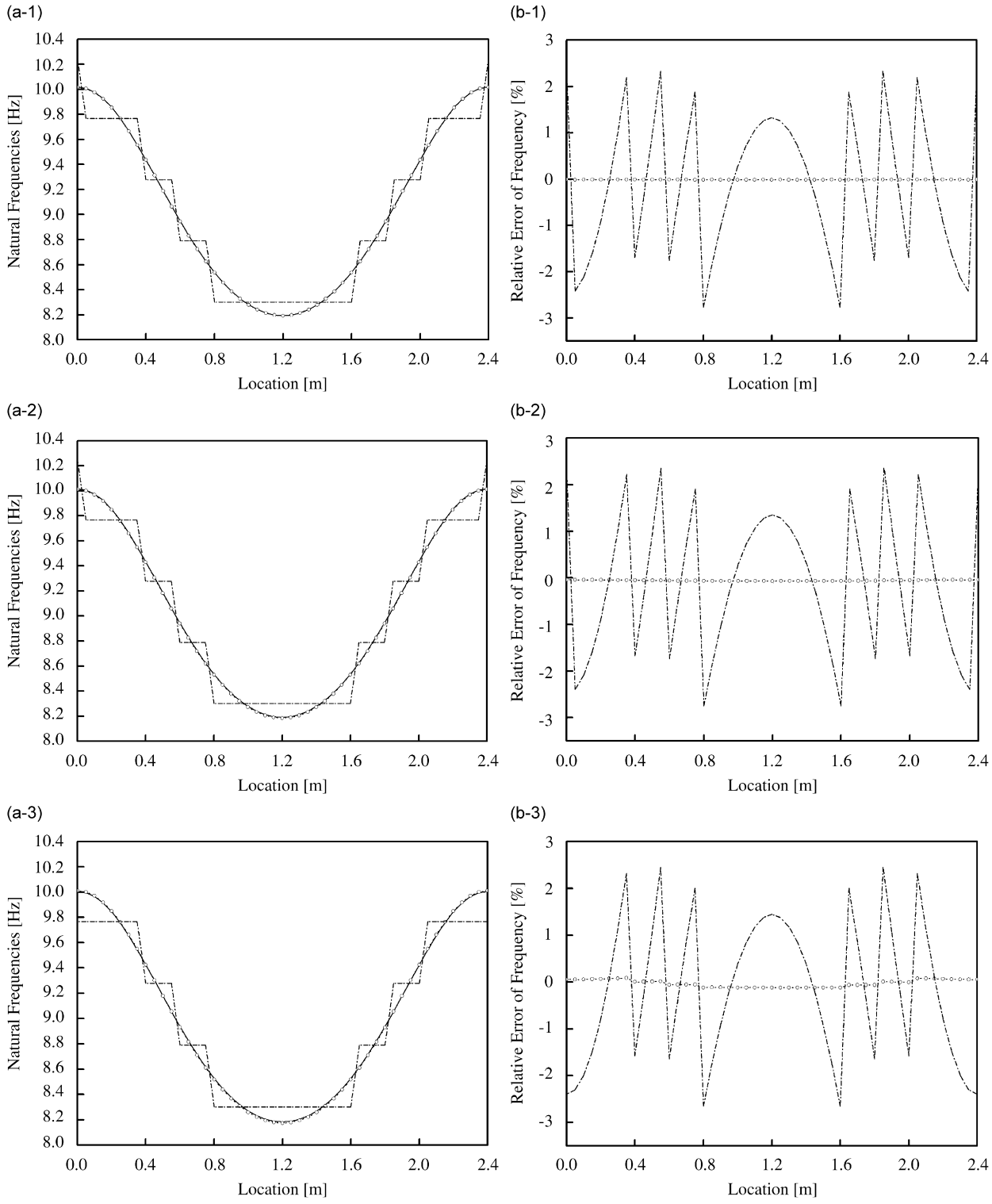

Fig. 9. (a) First natural frequency curves and (b) relative errors of frequency using FEM, SCCM and FFT for intact aluminium beams, for varying damping ratios ζ and with an auxiliary mass ($m = 4$ kg) spatial probing using different analysis methods: $\zeta = 0.02$ for (a-1) and (b-1); $\zeta = 0.05$ for (a-2) and (b-2); $\zeta = 0.10$ for (a-3) and (b-3); (——) frequency from FEM, (· · ·◇· · ·) frequency from SCCM of FFT data, and (– · – · – ·) frequency from FFT of response history.

However, the relative errors are less than 0.12% even if the beam has a high level of damping ($\zeta = 0.10$). The relative errors of frequencies calculated by FFT are shown in Fig. 9(b-1)–(b-3), and are seen to be greater than those calculated by SCCM. Therefore, SCCM can give a highly accurate estimate of the natural frequencies of beam-like structures by only using the response time history without the need to measure or determine the input excitation signal.

4. Damage detection in beam-like structures based on using modal frequencies derived by SCCM

It is difficult and in most cases impossible to detect and locate damage from purely a plot of the modal frequencies versus axial location of the auxiliary mass. To enhance the data, derivatives of the frequency curves are used. This method, in fact, is an application in structural damage detection of the derivatives of eigenvalues with respect to design parameters (or updating parameters). In this paper, the updating parameter of a beam with an auxiliary mass is the location of the mass along the beam. This kind of updating parameter cannot be found in any literature that have been published. The derivatives of eigenvalues (frequencies) with respect to the locations of an auxiliary mass along a beam have been investigated in this section for beam-like structure damage detection.

4.1. Illustration of proposed approach

The approach proposed in this paper for damage detection in beam-like structures is the use of the derivatives of the modal frequency curves. This is illustrated via a numerical example based on a cracked beam of dimensions $2400 \times 100 \times 25\,\text{mm}^3$ and whose crack depth, crack location and damping ratio are, respectively, $h_c = 5\,\text{mm}$, $l_c = 0.4\,\text{m}$ and $\zeta = 0.02$. The response time histories of the cracked beam were computed using the ABAQUS FEA programme. These response time histories were computed at spatial intervals of 50 mm along the length of the beam. The SCCM of the FFT of these response histories are computed and plotted against the axial locations of the mass.

Fig. 10(a) is the first natural frequency curve corrected by SCCM. From this figure, the first natural frequency curve of the cracked beam with an auxiliary mass is apparently a single smooth curve. Actually, due to the crack effect, the curve exhibits hidden local peaks or discontinuities in the region of damage which are not visible in Fig. 10(a). A very simple method to detect these, which is based on the use of the derivatives of the frequency curve, is proposed. The derivatives are expected to reveal the hidden aspect of the data. In the present work, the first three derivatives of the frequency curve, namely $(\mathrm{d}^n f/\mathrm{d}l_m^n)$, $n = 1, 2, 3$, are used to produce data for damage detection of beam-like structure. Fig. 10(b)–(d) show the first three derivatives of the first natural frequency curve corrected by SCCM. It is seen that the second and third derivatives provide a progressively better indication of the presence of a crack at 400 mm from the left end of the beam because the derivative curves exhibit significant discontinuity at this position.

To further verify the efficiency and practicability of the proposed method using the derivatives of the frequency curve, the effects of crack depth, auxiliary mass, damping ratio and random noise were also investigated. The findings are discussed in the following sub-sections.

4.2. Effects of crack depth

Fig. 11(a-1), (b-1), (c-1) and (d-1) are, respectively, the first natural frequency curve and the first, second and third derivatives of the frequency curve of cracked beams with damping ratio of $\zeta = 0.02$, whose crack location is $l_c = 0.4\,\text{m}$ and whose crack depths are 2.5, 5, 7.5, 10 and 12.5 mm. Also, a mass of $m = 4\,\text{kg}$ is traversed along the beam from one end to the other. Fig. 11(a-2)–(d-2) show the corresponding zoom curves of Fig. 11(a-1)–(d-1) around the crack location. From these figures, it is seen that the first three derivatives provide a progressively better indication of the presence of a crack at 0.4 m from the left end of the beam. For a deep crack (e.g. $h_c = 10$ or 12.5 mm), crack detection can be carried out from the first derivative of the natural frequency curve of the beam because there is an obvious discontinuity in the first derivative curve at the crack region. On the other hand, the second and third derivatives enable progressively smaller cracks to be identified. Also, from all the curves, one conclusion can be drawn that the deeper the crack, the greater the

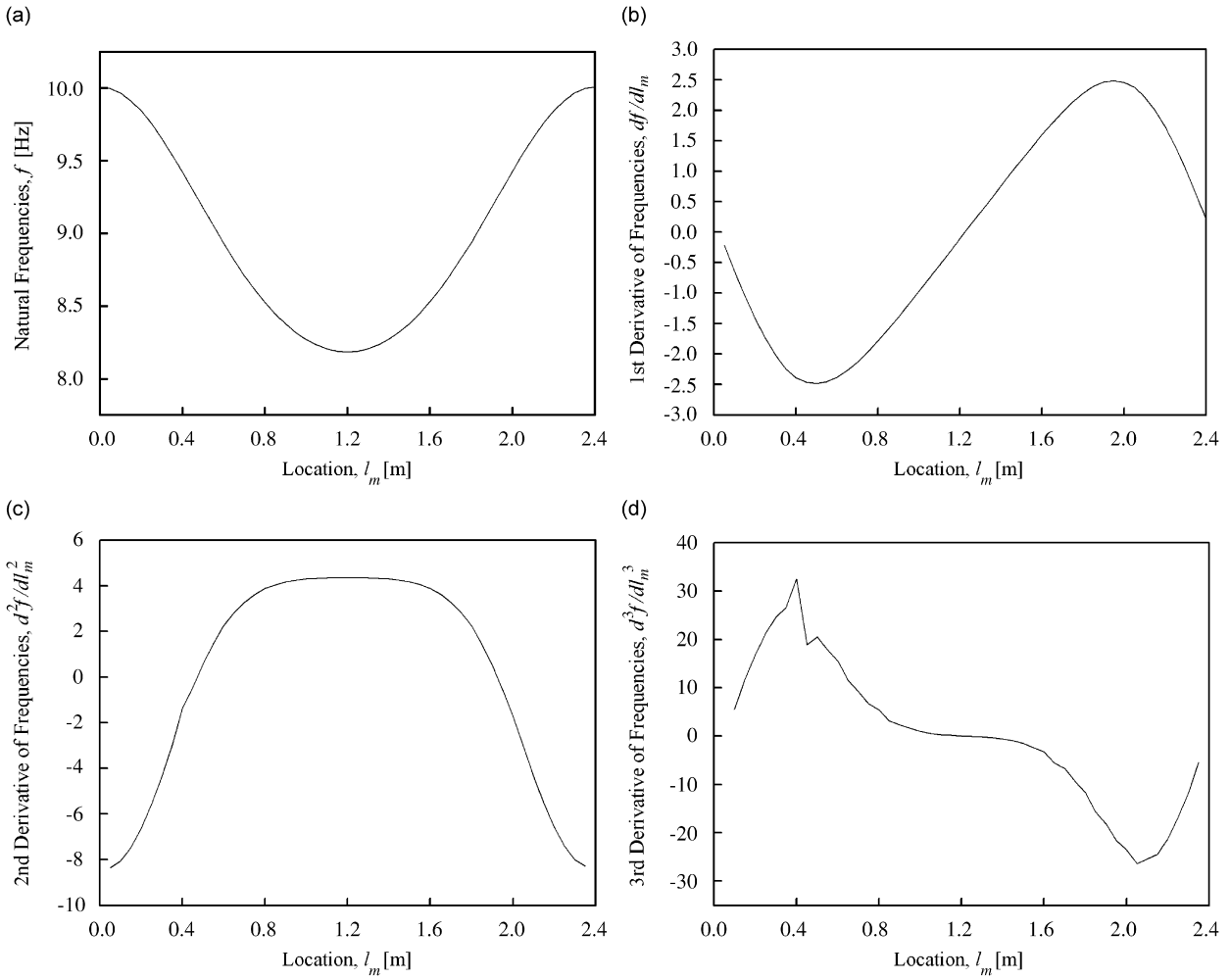

Fig. 10. Corrected first natural frequency curve by SCCM and its derivative for a cracked aluminium beam ($l_c = 0.4$ m, $h_c = 5$ mm, $\zeta = 0.02$) with an auxiliary mass ($m = 4$ kg) spatial probing: (a) first natural frequency curve; (b) first derivative; (c) second derivative; and (d) third derivative.

magnitude of the peak value of the derivatives of the natural frequency curve. That is, a more obvious crack indication is given.

4.3. *Effects of auxiliary mass*

In this section, the effects of auxiliary mass on the frequency curves are investigated. Auxiliary masses of magnitudes $m = 1, 2, 4, 6$ and 8 kg are traversed from one end of the cracked beam to the other. The beam has a damping ratio of $\xi = 0.02$, and a crack of depth $h_c = 5$ mm located at $l_c = 0.4$ m. Fig. 12(a)–(d) are, respectively, the first natural frequency curve and the first, second and third derivatives of the frequency curve of the cracked beam. Fig. 12(a) shows that the natural frequencies decrease when the auxiliary masses are traversed along the beam and that the natural frequencies decrease in magnitude as the magnitude of the auxiliary mass increases. Similarly, it can be seen from Fig. 12(a) to (d) that the first three derivatives provide a progressively better indication of the presence of a crack located at 0.4 m. Also, the derivative of the frequencies give better crack indication if the auxiliary mass increases in magnitude.

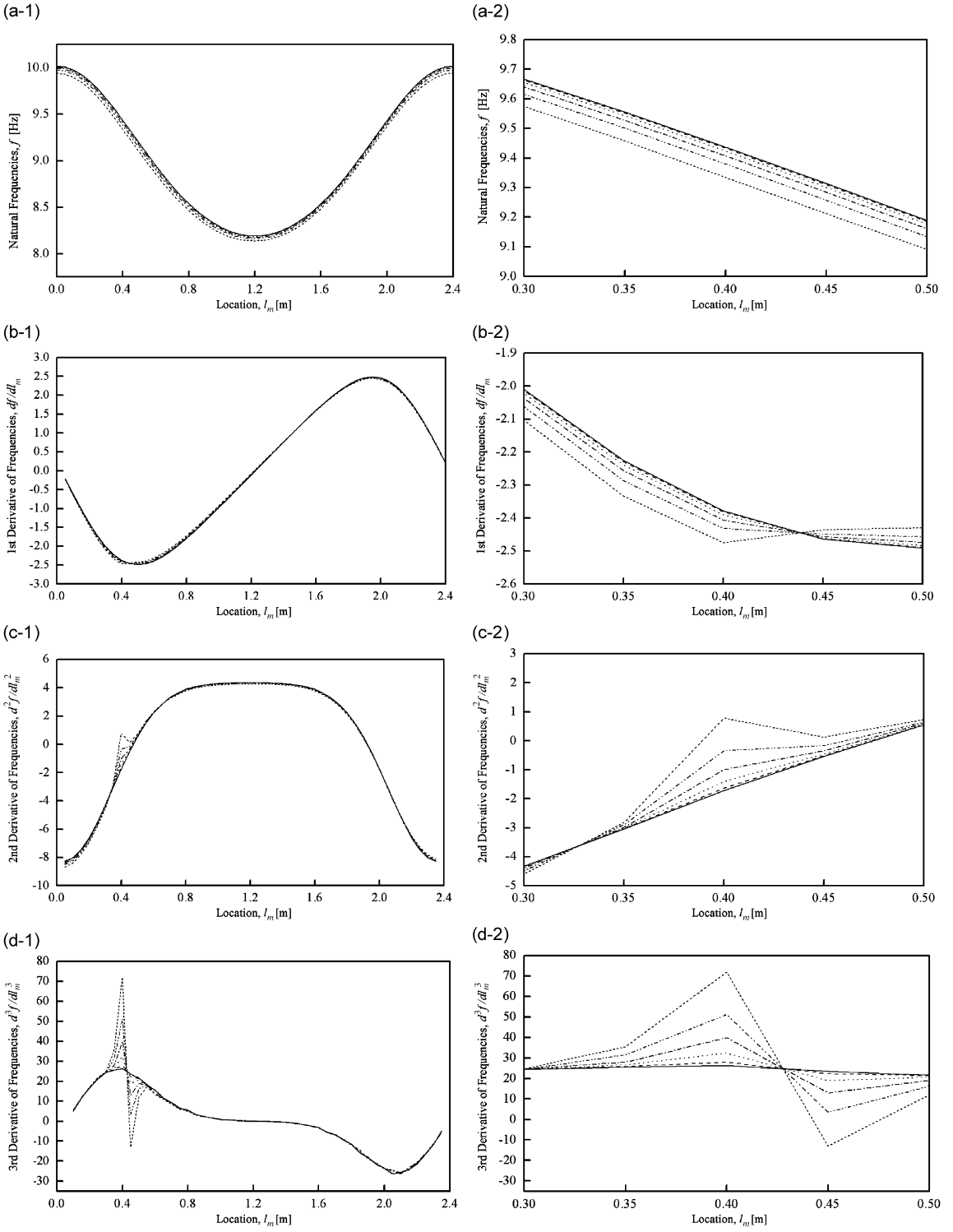

Fig. 11. Corrected first natural frequency curve by SCCM and its derivative for a cracked aluminium beam ($l_c = 0.4$ m, $\xi = 0.02$) with an auxiliary mass ($m = 4$ kg) and the corresponding zoom curves for varying crack depths: (a-1) first natural frequency curve, (b-1) first derivative, (c-1) second derivative, and (d-1) third derivative; (a-2)–(d-2) are the zoom curves of (a-1)–(d-1) around the crack location; (——) $h_c = 0$ mm (intact beam), (– – – –) $h_c = 2.5$ mm, (· · · · · ·) $h_c = 5$ mm, (–·–·–·–) $h_c = 7.5$ mm, (–··–··–··–) $h_c = 10$ mm, and (·····) $h_c = 12.5$ mm.

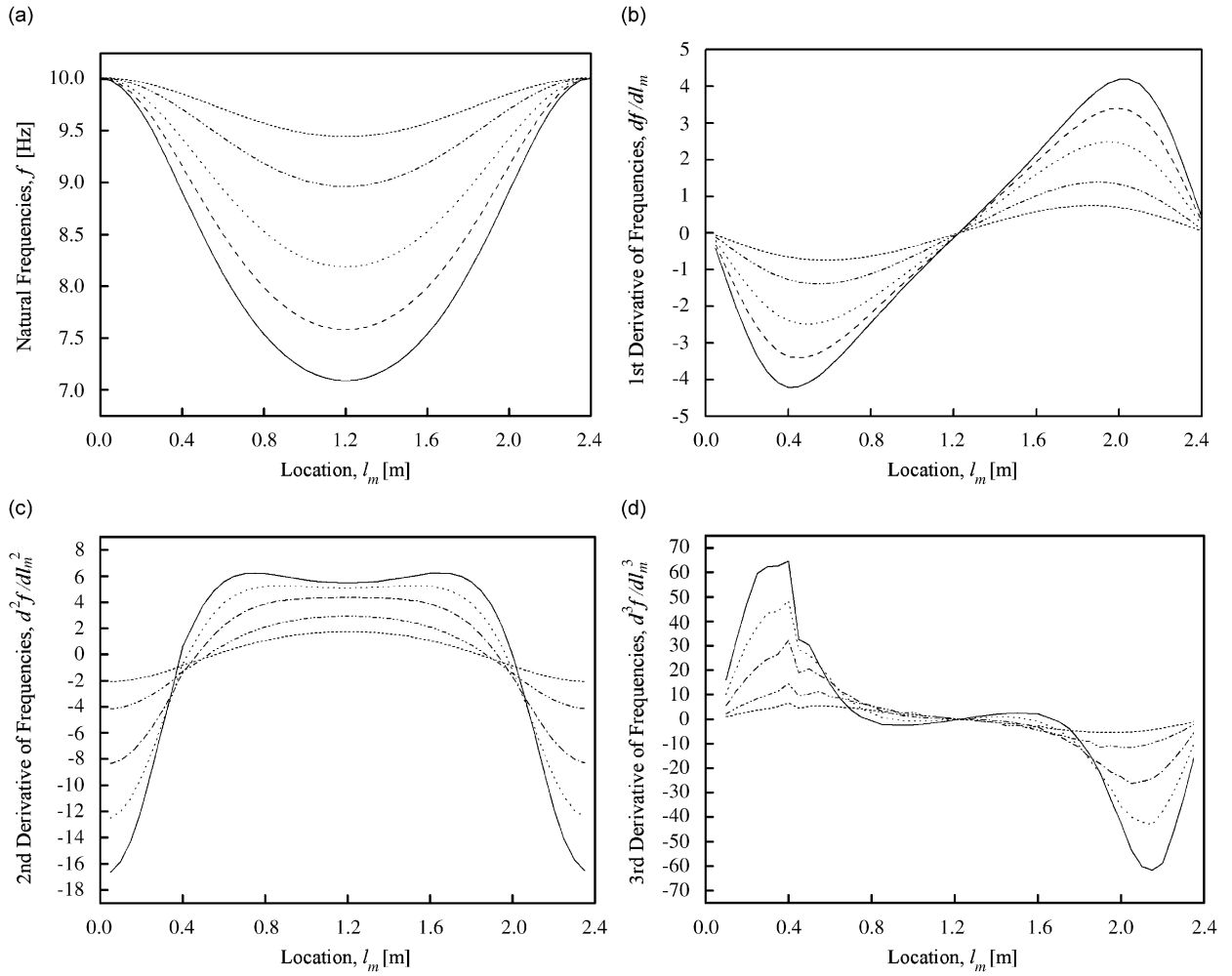

Fig. 12. Corrected first natural frequency curve by SCCM and its derivative of a cracked aluminium beam ($l_c = 0.4$ m, $h_c = 5$ mm, $\xi = 0.02$) with different auxiliary masses: (a) first natural frequency curve; (b) first derivative; (c) second derivative; and (d) third derivative; (·-------·) $m = 1$ kg, (–·–·–·) $m = 2$ kg, (· · · · · ·) $m = 4$ kg, (– – – –) $m = 6$ kg, and (——) $m = 8$ kg.

4.4. Effects of damping ratios

Three different damping ratios of the cracked beam, that is $\xi = 0.01$, 0.02, and 0.05, were investigated. Fig. 13(a)–(d) show the first natural frequency curve and the first, second and third derivative of the frequency curve, respectively, for the cracked beam whose crack location and crack depth are $l_c = 0.4$ m and $h_c = 7.5$ mm. Similar to the result given above, the first three derivatives provide a progressively better indication of the presence of a crack at 0.4 m from the left end of the beam. However, 'noise' effects due to the difference approximation error [34] begin to be magnified at the third derivatives of the natural frequency curve of the beam with the damping ratio of $\xi = 0.05$. Therefore, in real applications, it is not advantageous to go beyond the third derivatives of the natural frequency curve.

The relationship between the crack indicator, using the third derivative of the natural frequency curve, damping ratios and crack depths were investigated. Two cracked beams with cracks at $l_c = 0.4$ m and whose crack depths were $h_c = 5$ mm (B1) and $h_c = 12.5$ mm (B2) were analysed. Four different damping ratios, namely $\xi = 0.01$, 0.02, 0.05, and 0.10 are used. Fig. 14(a) and (b) show the third derivatives of corrected first natural frequency curves of the beam with a 5 mm deep crack and with four different damping ratios from 0.01

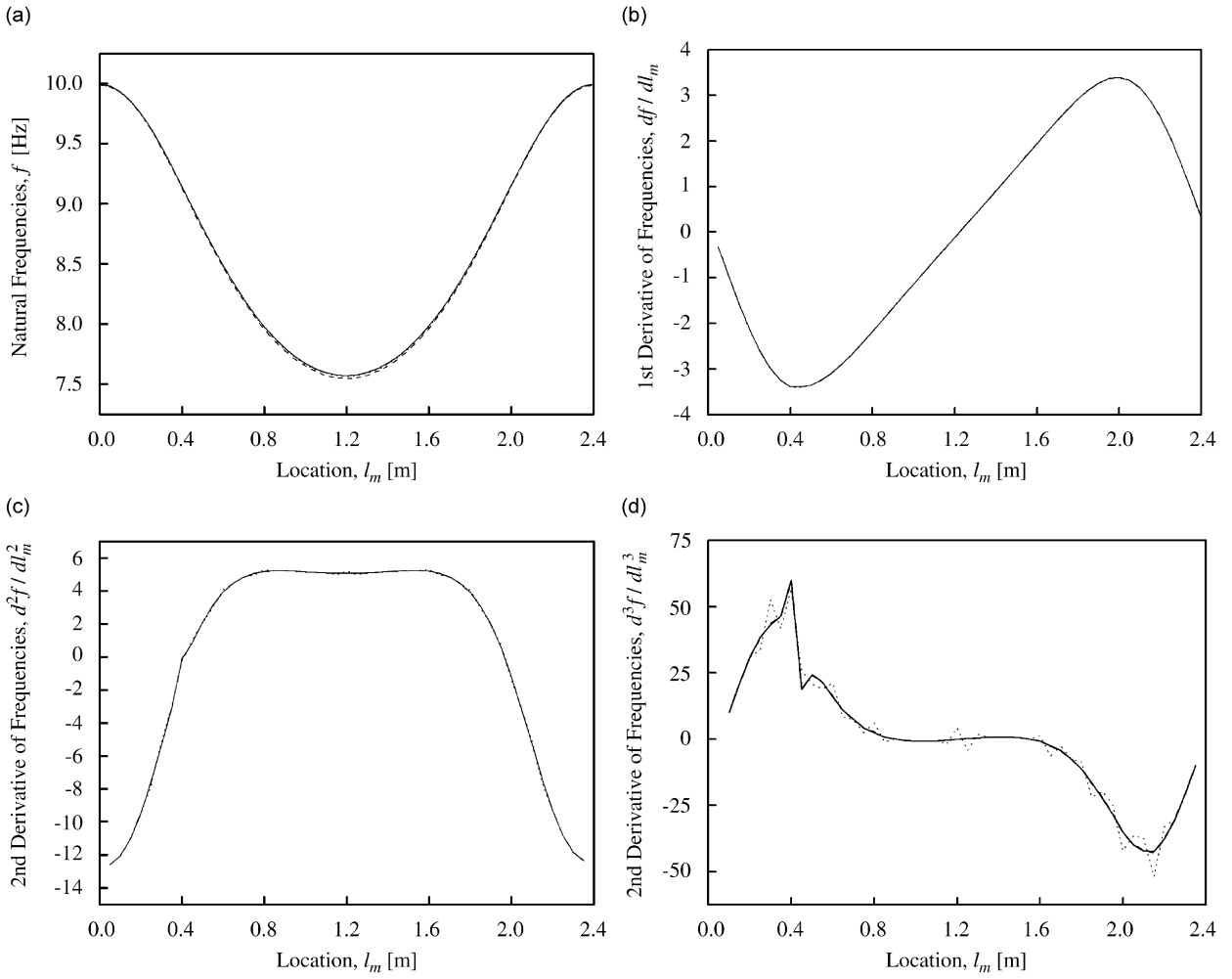

Fig. 13. Corrected first natural frequency curve by SCCM and its derivative of a cracked aluminium beam ($l_c = 0.4$ m, $h_c = 7.5$ mm) with an auxiliary mass ($m = 6$ kg): (a) first natural frequency curve; (b) first derivative; (c) second derivative; and (d) third derivative: (——) $\zeta = 0.01$, (– – – –) $\zeta = 0.02$, and (· · · · ·) $\zeta = 0.05$.

to 0.1. It can be seen that when the damping ratio is small (i.e. 0.01 and 0.02), the third derivative of the natural frequency curve provide clear indication of the presence of a crack at 0.4 m; when the damping ratio is large (i.e. 0.05 and 0.10), it is hard to obtain useful information from the third derivative of the natural frequency curve. However, for the beam with a 12.5 deep crack, when damping ratios are 0.01, 0.02 and 0.05, the third derivatives of the natural frequency curves provide clear information for crack identification and location. But when the damping ratio is 0.10, the crack cannot be clearly identified from the third derivative of the frequency curve. Therefore, one conclusion can be drawn that the deeper the crack, the more obvious the crack indicator using the third derivatives of the natural frequency curve. Also, when the damping ratio increases, the crack effect decreases such that the third derivatives of the natural frequency curve does not provide a clear indication of the crack.

At first sight, the results shown in Figs. 13 and 14 that the 'noise' associated with the third derivative increases as the damping increases look anomalous. However, a careful consideration shows that it is a correct behaviour. When the damping increases, the peak response of the structure at its resonance decreases. Therefore, the effects of noise on the peak response amplitude increase. Consequently, the 'noise' associated with the frequency estimates increases.

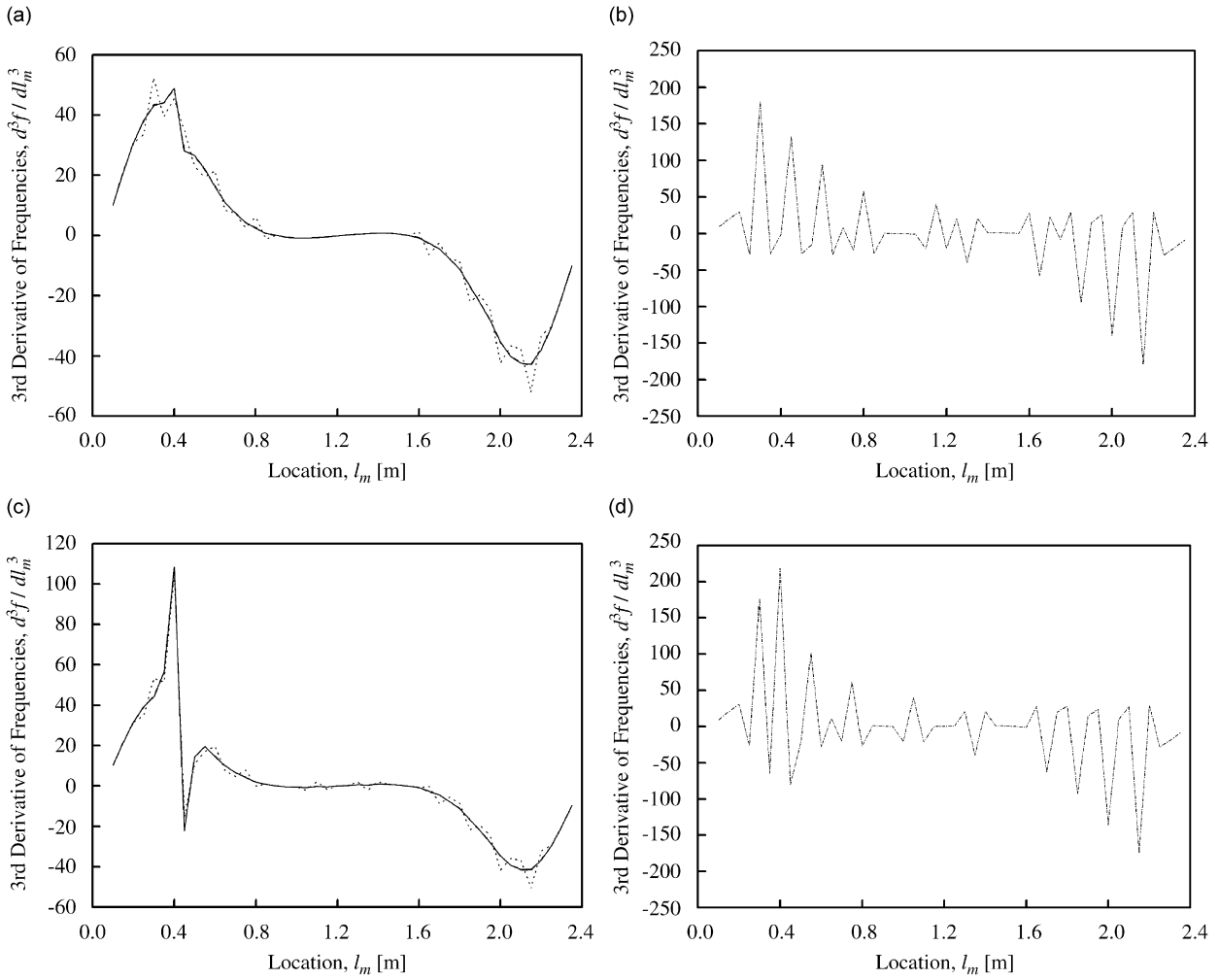

Fig. 14. The third derivative of the corrected first natural frequency curve of a cracked aluminium beam B1 ($l_c = 0.4$ m, $h_c = 5$ mm) and another cracked beam B2 ($l_c = 0.4$ m, $h_c = 12.5$ mm) with an auxiliary mass ($m = 6$ kg): (a) and (b) third derivative for B1, (c) and (d) third derivative for B2: (——) $\zeta = 0.01$, (– – – –) $\zeta = 0.02$, (· · · · ·) $\zeta = 0.05$, and (–·–·–) $\zeta = 0.10$.

4.5. *Effects of noise*

The above results are attributed to the fact that the analysed data are obtained from theoretical finite element computations of the response and hence contain no experimental noise. For real cases, experimental noise is expected to corrupt the response data and, hence, the natural frequencies of beam-like structures. In this section, response data with an associated normally distributed random noise was also studied. Normally distributed random noise of magnitudes 2% and 5% of root-mean-square (rms) of response data are added to the response data of beam-like structures. The natural frequencies were calculated as follows. Firstly, 32 segments of 2048-point continuous noisy signals were obtained. Secondly, average power spectrum was calculated by the FFT of the 32 signal segments. Then, the frequencies were calculated by SCCM of the result of the average power spectrum.

Fig. 15(a)–(d) are, respectively, the first natural frequency curve and the first, second and third derivatives of the frequency curve of the cracked beam whose crack location and crack depth are $l_c = 0.4$ m and $h_c = 7.5$ mm, respectively. Also, the beam was subjected to a mass of $m = 4$ kg traversed along the beam from one end to the other. Fig. 15(a) and (b) show that the natural frequencies and the first derivative, calculated

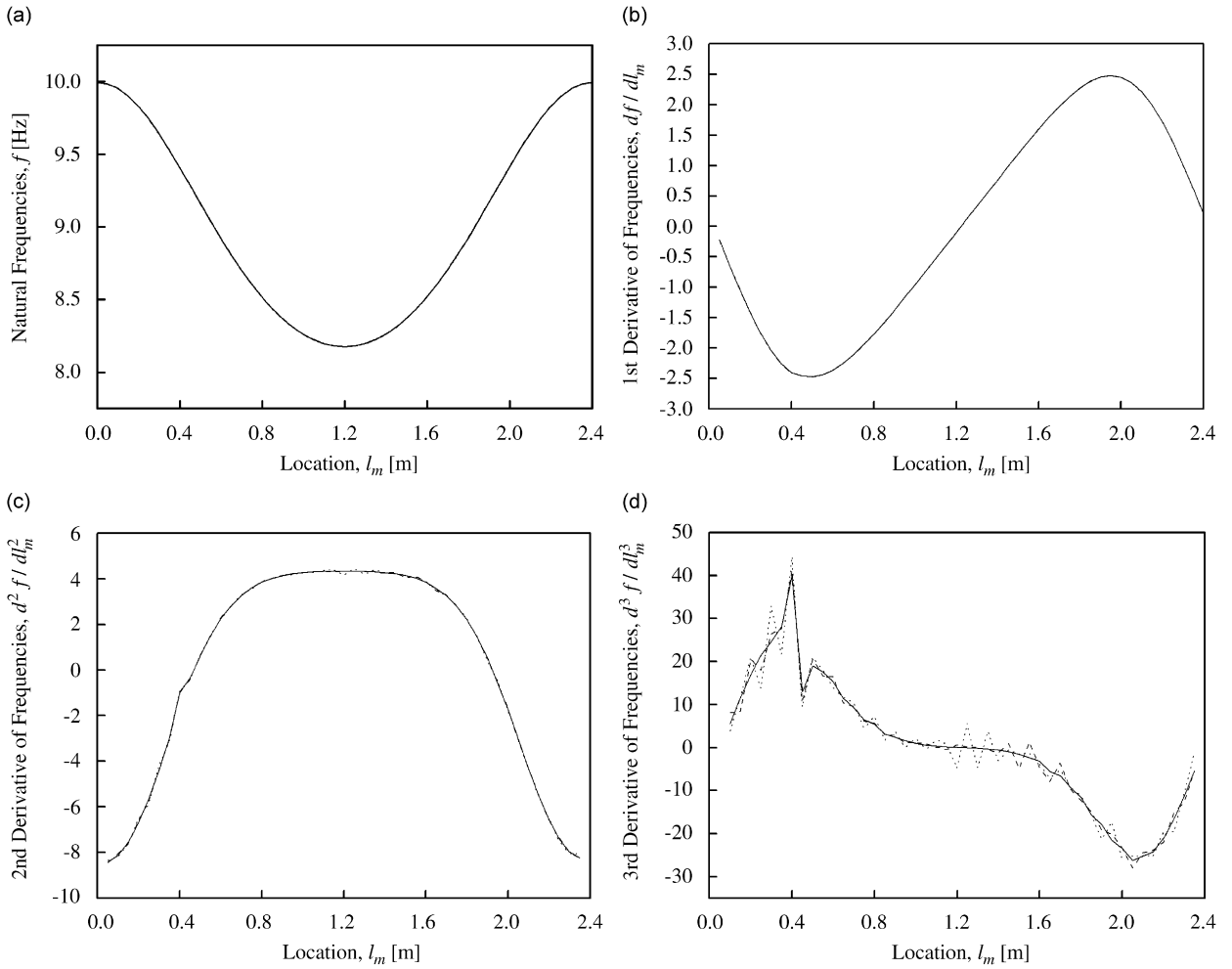

Fig. 15. First corrected noisy natural frequency curve by SCCM and its derivative of a cracked aluminium beam ($l_c = 0.4$ m, $h_c = 7.5$ mm, $\zeta = 0.02$) with an auxiliary mass ($m = 4$ kg): (a) first natural frequency curve; (b) first derivative; (c) second derivative; and (d) third derivative; (——) no noise, (– – – –) 2% noise, and (· · · · ·) 5% noise.

using SCCM from the response data without and with added random noise, are almost the same. This shows that the SCCM provides accurate frequency estimates even in the presence of noise. That is, the SCCM has a high anti-noise ability. The second derivatives of the frequency curves are smooth curves, from which crack detection can be made using the obvious discontinuity manifested at the crack region. However, the third derivative of the natural frequency curves of the beam is contaminated by the added noise. The noise associated with the third derivative curve for the case of 5% added noise is larger than that of 2%. Nevertheless, the second and third derivatives provide a progressively better indication of the presence of a crack at 0.4 m from the left end of the beam. However, it is not advantageous to go beyond the third derivatives of the natural frequency curve.

5. Concluding remarks

This paper proposes a new approach based on auxiliary mass spatial probing using the spectral centre correction method (SCCM), to provide a simple solution for damage detection by just using the response time history of beam-like structure. The natural frequencies of a damaged beam with a traversing auxiliary mass change due to change in flexibility and inertia of the beam as the auxiliary mass is traversed along the beam.

Therefore the auxiliary mass can enhance the effects of the crack on the dynamics of the beam and, therefore, facilitate the identification and location of damage in the beam. That is, the auxiliary mass can be used to probe the dynamic characteristics of the beam by traversing the mass from one end of the beam to the other.

However, it is impossible to obtain accurate modal frequencies by the direct operation of the fast Fourier transform (FFT) procedure on the response data of the structure because the frequency spectrum can be only calculated for sampling limited time data which results in the well-known leakage effect. SCCM is identical to the energy centrobaric correction method (ECCM) which is a practical and effective method to overcome the shortcoming of the FFT in order to provide highly accurate estimates of frequency.

From the modal responses of damaged simply supported beams with auxiliary mass computed using the finite element method (FEM), graphical plots of the natural frequencies calculated by SCCM versus axial location of auxiliary mass were obtained. It was shown that it is difficult to locate a crack directly from these natural frequency curves. Therefore, a practical method, which is based on the derivatives of natural frequency curves was proposed. It was shown that the method enables clear and unambiguous identification and location of cracks in a beam-like structure. The efficiency and practicability of the proposed method was illustrated via numerical simulation.

For real cases, however, experimental noise is expected to corrupt the response data and, hence, the natural frequencies of beam-like structures. Consequently, the effect of noise was also investigated. In real applications, it is suggested that average power spectrum be used in order to reduce the noise effect. Also, the effects of crack depth, auxiliary mass and damping ratios were investigated. The results show that the deeper the crack, the greater the magnitude of the peak value of the derivative of the natural frequency curve; the derivatives of the natural frequency curves give better crack indication if the auxiliary mass increases in magnitude; also, the crack effect decreases when the damping ratio increases. From the simulated results, the efficiency and robustness of the proposed method has been demonstrated. Also, the proposed method has low computational cost and high precision and it is, therefore, recommended for real applications.

Acknowledgement

The award of a University of Manchester ‘University Scholarship’ to Shuncong Zhong is gratefully acknowledged.

References

[1] Z. Duan, G. Yan, J.P. Ou, B.F. Spencer, Damage localization in ambient vibration by constructing proportional flexibility matrix, *Journal of Sound and Vibration* 284 (2005) 455–466.
[2] E. Parloo, P. Verboven, P. Guillaume, M. Van Overmeire, Autonomous structural health monitoring, Part II: vibration-based in-operation damage assessment, *Mechanical Systems and Signal Processing* 16 (4) (2002) 659–675.
[3] E. Parloo, S. Vanlanduit, P. Guillaume, P. Verboven, Increased reliability of reference-based damage identification techniques by using output-only data, Journal of Sound and Vibration 270 (2004) 813–832.
[4] Y. Lu, F. Gao, A novel time-domain auto-regressive model for structural damage diagnosis, *Journal of Sound and Vibration* 283 (2005) 1031–1049.
[5] S. Choi, N. Stubbs, Damage identification in structures using the time-domain response, *Journal of Sound and Vibration* 275 (2004) 577–590.
[6] Y. Narkis, Identification of crack location in vibrating simply supported beams, *Journal of Sound and Vibration* 172 (1994) 549–558.
[7] A. Messina, I.A. Jones, Damage detection and localization using natural frequency change, *14th International Modal Analysis Conference*, Orlando, 1996, pp. 67–76.
[8] A. Messina, E.J. Williams, T. Contursi, Structural damage detection by sensitivity and statistical-based method, *Journal of Sound and Vibration* 216 (5) (1998) 791–808.
[9] O.S. Salawu, Detection of structural damage through changes in frequencies: a review, *Engineering Structures* 19 (1997) 718–723.
[10] Y.S. Lee, M.J. Chung, A study on crack detection using eigenfrequency test data, *Computers and Structures* 77 (2000) 327–342.
[11] L.J. Hadjileontiadis, E. Douka, A. Trochidis, Crack detection in beams using kurtosis, *Computers and Structures* 83 (2005) 909–919.
[12] M. Xie, K. Ding, Correction methods in spectrum analysis, *Journal of Vibration Engineering* 7 (2) (1994) 172–179.
[13] D.S. Huang, Phase error in fast Fourier transform analysis, *Mechanical System and Signal Processing* 9 (1995) 113–118.
[14] K. Ding, M. Xie, Three-point convolution correction method for discrete spectrum, *Journal of Vibration Engineering* 9 (1) (1996) 92–98.

[15] X. Ming, D. Kang, Corrections for frequency, amplitude and phase in a fast Fourier transform of a harmonic signal, *Mechanical System and Signal Processing* 10 (1996) 211–221.
[16] D. Kang, X. Ming, Z. Xiaofei, Phase difference correction method for phase and frequency in spectral analysis, *Mechanical System and Signal Processing* 14 (5) (2000) 835–843.
[17] K. Ding, S. Zhong, X. Zhu, A comparative study of phase difference correcting method on discrete spectrum, *Journal of Vibration and Shock* 20 (2) (2001) 19–26 (in Chinese).
[18] K. Ding, S. Zhong, A universal phase difference correction methods on discrete spectrum, *Acta Electronica Sinica* 31 (1) (2003) 142–145.
[19] K. Ding, L. Jiang, Energy centrobaric correction method for discrete spectrum, *Journal of Vibration Engineering* 14 (3) (2001) 354–358 (in Chinese).
[20] L. Zhu, Y. Xiong, B. Zhong, An approach for amplitude correction in line spectrum, *Mechanical System and Signal Processing* 17 (3) (2003) 551–560.
[21] K. Ding, W. Li, X. Zhu, *Fault Diagnosis Technology in Gear and Gearbox*, China Machine Press, Beijing, 2005.
[22] A.K. Pandey, M. Biswas, M.M. Samman, Damage detection from changes in curvature mode shapes, *Journal of Sound and Vibration* 145 (2) (1991) 321–332.
[23] M.M. Abdel Wahab, G. De Roeck, Damage detection in bridges using modal curvatures: application to a real damage scenario, *Journal of Sound and Vibration* 226 (2) (1999) 217–235.
[24] W.H. Wittrick, Rates of change of eigenvalues, with reference to buckling and vibration problems, *Journal of the Royal Aeronautical Society* 66 (1962) 590–591.
[25] R.L. Fox, M.P. Kapoor, Rates of change of eigenvalues and eigenvectors, *Journal of AIAA* 6 (12) (1968) 2426–2429.
[26] R.B. Nelson, Simplified calculation of eigenvector derivatives, *AIAA Journal* 14 (9) (1976) 1201–1205.
[27] M.I. Friswell, Calculation of second and higher order eigenvector derivatives, *Journal of Guidance, Control, and Dynamic* 18 (4) (1995) 919–921.
[28] M.I. Friswell, J.E. Mottershead, *Finite Element Model Updating in Structural Dynamic*, Kluwer Academic Publishers, Dordrecht, 1996.
[29] A.L. Andrew, Iterative computation of derivatives of eigenvalues and eigenvectors, *IMA Journal of Applied Mathematics* 24 (1979) 209–218.
[30] C.E. Roger, Computing derivatives of eigenvalues and eigenvectors by simultaneous iteration, *IMA Journal of Numerical Analysis* 9 (1989) 111–122.
[31] S. Adhikari, Rates of change of eigenvalues and eigenvectors in damped dynamic system, *Journal of AIAA* 37 (11) (1999) 1452–1458.
[32] K.M. Choi, S.W. Cho, M.G. Ko, I.W. Lee, Higher order eigensensitivity analysis of damped systems with repeated eigenvalues, *Computers and Structures* 82 (2004) 63–69.
[33] L.M. Zhu, H.X. Li, H. Ding, Estimation of multi-frequency signal parameters by frequency domain non-linear least squares, *Mechanical System and Signal Processing* 19 (2005) 955–973.
[34] R.W. Southworth, Digital Computation and Numerical Methods, New York, 1965.